Published in final edited form as:

Prog Retin Eye Res. 2024 March ; 99: 101232. doi:10.1016/j.preteyeres.2023.101232.

IOP and glaucoma damage: The essential role of optic nerve head and retinal mechanosensors

Ian Pitha[a,b,c], **Liya Du**[a], **Thao D. Nguyen**[a,d], **Harry Quigley**[a,c,*]

[a]Department of Ophthalmology, The Johns Hopkins University School of Medicine, Baltimore, MD, USA

[b]Center for Nanomedicine, The Johns Hopkins University School of Medicine, Baltimore, MD, USA

[c]Glaucoma Center of Excellence, The Johns Hopkins University School of Medicine, Baltimore, MD, USA

[d]Department of Mechanical Engineering, The Johns Hopkins University, Baltimore, MD, USA

Abstract

There are many unanswered questions on the relation of intraocular pressure to glaucoma development and progression. IOP itself cannot be distilled to a single, unifying value, because IOP level varies over time, differs depending on ocular location, and can be affected by method of measurement. Ultimately, IOP level creates mechanical strain that affects axonal function at the optic nerve head which causes local extracellular matrix remodeling and retinal ganglion cell death – hallmarks of glaucoma and the cause of glaucomatous vision loss. Extracellular tissue strain at the ONH and lamina cribrosa is regionally variable and differs in magnitude and location between healthy and glaucomatous eyes. The ultimate targets of IOP-induced tissue strain in glaucoma are retinal ganglion cell axons at the optic nerve head and the cells that support axonal function (astrocytes, the neurovascular unit, microglia, and fibroblasts). These cells sense tissue strain through a series of signals that originate at the cell membrane and alter cytoskeletal organization, migration, differentiation, gene transcription, and proliferation. The proteins that translate mechanical stimuli into molecular signals act as band-pass filters – sensing some stimuli while ignoring others – and cellular responses to stimuli can differ based on cell type and differentiation state. Therefore, to fully understand the IOP signals that are relevant to glaucoma, it is necessary to understand the ultimate cellular targets of IOP-induced mechanical stimuli and their ability to sense, ignore, and translate these signals into cellular actions.

[*]Corresponding author. Department of Ophthalmology, The Johns Hopkins University School of Medicine, Baltimore, MD, USA. hquigley@jhmi.edu (H. Quigley).

CRediT authorship contribution statement

Ian Pitha: Conceptualization, Writing – original draft, Writing – review & editing. **Liya Du:** Writing – original draft, Writing – review & editing. **Thao D. Nguyen:** Conceptualization, Writing – original draft, Writing – review & editing. **Harry Quigley:** Conceptualization, Writing – original draft, Writing – review & editing.

1. Introduction

While it has been at least suspected for nearly 400 years that intraocular pressure (IOP) is related to glaucoma (Keeler et al., 2013), the nature of this association has been obscured by fixed ideas and a limited ability to measure key parameters. These roadblocks that cloud our understanding include: 1) the single point in time measurement of IOP by tonometry is indicative of mean IOP or its short-term variance; 2) the mean tonometric IOP measured a handful of times per year represents the risk factor accurately; 3) IOP must be higher than some arbitrary value ("normal") to be dangerous; 4) variations in IOP (second to second, minute to minute, diurnally) may be relevant, but are not important clinically; 5) reducing IOP to the range present in most non-glaucoma eyes in a population (normalizing IOP) is a satisfactory treatment goal.

Our historical understanding of the IOP/glaucoma relation was significantly informed by the development of relatively accurate tonometers (Friedenwald and Moses, 1950; Goldmann, 1954), use of gonioscopy (Barkan, 1954), the quantitative assessment of optic nerve damage in photos/images and functional testing, and particularly population-based studies (Hollows and Graham, 1966; Sommer et al., 1991) that showed the full spectrum of glaucomatous optic neuropathy rather than only among persons presenting to health care. Typical of these advances was the recognition in the early 20th century that asymptomatic open angle glaucoma (OAG) was an entity associated with various levels of IOP. Prior to that time, glaucoma was the term applied only to eyes symptomatic from extreme IOP levels (angle closure or secondary glaucoma) (Curran, 1920; Rosengren, 1950). However, the causal relationship for all glaucomas was still stressed as "elevated" IOP (Jensen and Maumenee, 1973).

Drance initially popularized the concept that OAG occurring in eyes with IOP in the normal range was fundamentally distinct, leading to the fallacy still commonly believed that "if the IOP is normal, something else must be causing glaucoma damage" (Drance, 1972). Yet, randomized trials have shown that lowering of IOP slows glaucoma damage regardless of whether baseline IOP is normal or elevated (Heijl et al., 2002; Leske et al., 1999). Whether there are distinct phenotypes of OAG based on prevailing untreated IOP is possible, but controversial. Despite editorials condemning the term low tension glaucoma, it survives in the literature (Sommer, 2011). There are many contributing risk factors for glaucomatous optic neuropathy (Leske, 2007), but here we will evaluate those that relate to IOP-generated stress.

Glaucomatous optic neuropathy can be defined by the combination of an excavated optic nerve head (ONH) and concomitant defects in visual field testing (Iyer et al., 2021), and modern definitions do not include the level of IOP. The death of retinal ganglion cells (RGC) is recognized as its primary pathological process (Kendell et al., 1995; Quigley and Green, 1979), and research has defined the type and rate of RGC loss both structurally (Bussel et al., 2014; Medeiros et al., 2012) and functionally (Harwerth et al., 2010; Heijl et al., 2013). A primary abnormality in RGC axons occurs in glaucoma at the ONH, where both anterograde and retrograde axonal transport are interrupted (Crish et al., 2010; Minckler et al., 1978; Pease et al., 2000; Quigley and Addicks, 1980; Quigley et al., 1982;

Salinas-Navarro et al., 2010). The physical reconfiguration at the ONH lamina cribrosa (LC) in glaucoma explains the selective loss of RGC axons at the upper and lower ONH (Emery et al., 1974; Quigley and Addicks, 1981; Radius et al., 1978).

In this review we will address two unresolved questions in the association between IOP and glaucoma: 1) what aspects of the IOP are important in producing glaucoma damage, and 2) how do the ocular mechanisms of response to IOP potentially lead to RGC damage?

2. What are the features of IOP?

While IOP may seem a straightforward parameter, it is substantially more complex than might be immediately evident (Fig. 1). As used clinically, the common unit of millimeters of mercury (mm Hg) is actually a pressure difference between inside the eye and atmospheric pressure. Standard atmospheric pressure at sea level is 100 KPa, while 15 mm Hg (the standard eye pressure as measured) is a difference of only 2 KPa above atmospheric. There is no single IOP in an eye at one point in time. The features leading to a measured IOP involve multiple dynamic physiological events. With respect to flow of aqueous humor, its contribution to IOP depends upon: 1) formation at the ciliary body, 2) flow with net direction anteriorly through the pupil, 3) outflow from both the trabecular meshwork and the uveoscleral tract, 4) evaporation of tear film from the cornea (Mishima and Maurice, 1961), and 5) aqueous diffusion through the vitreous cavity to retina and optic nerve head. If the pressure differential between any location within the eye and atmospheric pressure were made with multiple sensors, a variety of IOPs would be detected. This is obvious from the fact that there are net flows in several directions. For example, the posterior to anterior chamber IOP difference is dependent on resistance through the iris—lens channel and can represent up to 8 mm Hg higher behind than in front of the iris in smaller eyes (Silver and Quigley, 2004). Pederson experimentally measured monkey IOP at different points within the eye and found it to be lower in the suprachoroidal space than near the ciliary body/sclera interface, which was lower than anterior chamber pressure (Emi et al., 1989). If there is net fluid flow, there will be pressure differences within the eye. For the purposes of specifying the relation to glaucoma, we need to account for which IOP and what aspects of IOP variation are relevant.

Tonometers used clinically report an IOP that is dependent upon their mechanism of action. The Goldmann applanation tonometer produces a relatively constant pressure on the cornea, visually averaged over several seconds and representing IOP indicative of anterior chamber IOP, modified by corneal thickness (Brandt, 2004) and viscoelasticity. Devices such as the TonoPen, Ocular Response Analyzer, and iCare instruments deliver a variety of forces to the cornea over only milliseconds, while the pneumatonograph shows a continuous output of ocular pulsation generated by a continuous and considerably larger pressure from the tonometer tip. The pulsatile change in IOP derives from the effect of arterial systole/diastole, largely in choroidal arteries, as modified by the corneoscleral connective tissues (Jin et al., 2018). Further vascular contributions to dynamic IOP are the outflow resistance in episcleral and vortex veins. The latter allow expansion of the choroid at lower IOP and its contraction at higher IOP (Maul et al., 2011). All tonometers indicate an anterior IOP, while the IOP-generated stress at the posterior site of glaucoma damage may be due to

either higher or lower IOP. Thus, our view of IOP and clinical decisions are determined not only by dynamic features of ocular physiology, but by the methods used to measure it. It is clear that IOP, typically estimated at the anterior chamber, varies in height, mean value, and variation over shorter and longer periods (Fig. 1). Since glaucoma damage to RGC axons occurs at the optic nerve head, posterior IOP is more relevant.

Short-term IOP variations can be dramatic. Recent studies have measured moment-to-moment IOP or its surrogates, using transducers connected to intraocular tubing in monkeys (Jasien et al., 2019), pressure sensitive devices implanted in human eyes (Szurman et al., 2023), and instrumented contact lenses (Flatau et al., 2016). The pneumatonographic IOP, measured at the cornea, and monkey transducer studies show the sinusoidal IOP variation due to the vascular pulsation. In addition, the monkey data show substantial, short-term increases due to blinks and eye movements. During sleep (Downs, 2015; Downs et al., 2011a), the horizontal body position causes IOP increase due to the rise in venous outflow resistance (Yang et al., 2020). Interestingly, monkey eyes have dramatically lower variability in IOP recordings during sleep, possibly due to their sleeping in a sitting position. The rise during sleep in humans is largely due to change in posture, not to diurnal change in corneal properties (Bagga et al., 2009), nor to altered outflow facility (Sit et al., 2008), and occurs despite a decrease in aqueous production and flow at night (Brubaker, 1991). Some data from corneal contact lenses suggest that it is the peaks of change in limbal curvature (imputed as IOP) that are associated with the presence of glaucoma or its past progressive worsening (De Moraes et al., 2018; Flatau et al., 2018). However, these are not the <1 s jumps seen with blinks, but rather are values taken minutes apart. Recent development of a home tonometer has shown greater variability in IOP throughout waking hours than would be imputed from measurements during typical office hours (McGlumphy et al., 2021).

In the past, it was common for clinicians to perform in-office IOP measurements through the course of one day or even with hospital admission to estimate diurnal IOP variation (Shuba et al., 2007). Such diurnal variation is often included in new IOP-lowering drug trials (Camras et al., 1998), but its value in predicting future glaucoma worsening has been questioned, since the pattern is not highly repeatable within glaucoma subjects (Realini et al., 2011). IOP measures in office practice are most often taken only 2–4 times per year. Such sparse sampling cannot capture the variation in minutes, hours, or diurnally. Yet, the literature deals with the standard deviation of infrequent office measurements as “fluctuation” (Nouri-Mahdavi et al., 2004) that may be indicative of disease-related IOP variability. This practice ignores the other factors that could determine such variance. Newer tools allow patients to measure eye pressure at home and have the potential to increase the number of IOP measurements that guide clinical management from isolated measurements taken once every several months to multiple daily measurements. The role and significance of this type of IOP monitoring, however, has not been established fully in clinical management of glaucoma patients.

Implantation of telemetric IOP sensors in animal models allows near continuous monitoring of IOP over time. In normotensive, non-human primates, telemetric IOP monitoring showed IOP fluctuations up to 10 mmHg in magnitude from hour-to-hour and day-to day (Downs et al., 2011a). When IOP was monitored on a second-to-second timescale, IOP fluctuations

due to ocular saccades, blinks, vascular filling, stress, and eye rubbing were documented and could be dramatic in magnitude (>100 mmHg elevation in the case of eye rubbing) (Downs et al., 2011a; Turner et al., 2019a, 2019b). Chronic monitoring using these sensors revealed cyclic changes in mean IOP as well as a pattern of the frequency of transient IOP variations that cycled over 16- to 91-days (Jasien et al., 2019). In a non-human primate glaucoma model maximum IOP was the best predictor of glaucomatous structural changes rather than mean IOP and IOP variability (over 1–3 weeks) (Gardiner et al., 2012). Again, the significance of many of these transient and cyclical variations has not been established in glaucoma.

Since all human eyes have moment-to-moment and diurnal/sleep related variance in IOP, these would only be relevant to glaucoma causation if the variances were greater in glaucoma eyes, or, if the glaucoma eye were more sensitive to variances tolerated by non-diseased eyes. Indeed, it has been shown that the variability of office-based IOP is greater in glaucoma eyes, and that the variance is reduced along with mean IOP by glaucoma filtering surgery (Wilensky et al., 1994). Yet, medical treatment may induce greater variability in IOP due to incomplete adherence with topical IOP-lowering drugs, which is unfortunately common. Due to the fact that IOP has a floor-effect and under physiological conditions does not go lower than episcleral venous pressure, eyes that have higher mean IOP with a normal EVP will also have greater variance. Whether glaucomatous eyes have more dynamic IOP variance over shorter time periods needs to be further studied. We can estimate the timescales or parameter limits that occur in adult human IOP. Mean IOP can range from 3 to 80 mm Hg, frequency of variation can be in the range of 1 cycle per second (blinks, saccades, cardiac cycles) to much longer intervals, as in minute to minute, diurnal, and even seasonal effects. The rate and degree of IOP change may be important. The levels and change in IOP that are important in glaucoma will ultimately depend upon the mechanisms by which the eye tissues and cells sense and respond to them.

3. Features of glaucomatous optic neuropathy

Study of experimental monkey and human glaucoma optic nerve heads shows that damage to RGC axons occurs at the LC (Anderson and Hendrickson, 1974; Quigley and Anderson, 1976; Quigley et al., 1981). The corresponding location in rodent eyes is also the site of injury, the unmyelinated optic nerve (Howell et al., 2007). The majority of RGCs produced *in utero* die by apoptosis due to failure to reach an appropriate target neuron (Perry et al., 1983). RGC that synapse with correct partners are sustained by continuous receipt of neurotrophic factors that repress the apoptosis (Raff et al., 1993). One mechanism of RGC death in glaucoma is recapitulation of this programmed cell death mechanism due to axonal transport blockade of neurotrophins (Quigley et al., 1995). In both animal models and human glaucoma, there is selective loss of RGC with sparing of other retinal neurons, including amacrines (Kielczewski et al., 2005) or photoreceptors (Kendell et al., 1995).

RGC axons remain unmyelinated until the posterior limit of the LC in monkey and human eyes, while myelination begins ~1 mm behind the eye in rodents. At the LC, RGC axons are separated into bundles by astroglial columns at the level of the choroid and by connective tissue beams lined by astrocytes at the scleral level, with beams

undergoing thickening during aging (Quigley, 1977b). The connective tissue beams in the LC contain collagens, elastin, glycoprotein matrix, fibroblasts, and the capillaries supplying local nutrition (Elkington et al., 1990; Hernandez et al., 1987, 1988). At the LC, mechanical stresses are directed both circumferentially from the peripapillary sclera (hoop stress) and by the trans-LC pressure differential between IOP and myelinated optic nerve tissue pressure (Burgoyne et al., 2005). The ultimate upstream mechanisms that underly RGC death and glaucomatous vision loss are multifactorial, involving neuroinflammation, astrocyte activation, mitochondrial function, and vascular dysregulation (Quigley, 2016; Weinreb et al., 2014). Each of these elements have mechanosensitive sensors that respond to IOP-generated stress that will be considered individually.

It is useful to consider which alterations in the LC are generated by pressure-induced stress and which are simply a result of the death of RGC axons. To do this, research has compared the differences between non-glaucoma optic neuropathy and glaucoma, both in human disease and in experimental models. In human glaucoma LC, there is a remodeling of the connective tissue beams and astrocyte positions that is not observed in other disorders causing RGC axon loss (Quigley and Green, 1979). Likewise, in experimental monkey glaucoma, connective tissue beams of the LC were dramatically remodeled (Quigley and Addicks, 1980), which did not occur after experimental optic nerve transection (Quigley and Anderson, 1977). These fundamental differences are visible in the characteristic clinical features of glaucoma compared to neuropathy at the same site not due to IOP-induced change (e.g. non-arteritic ischemic optic neuropathy) (Danesh-Meyer et al., 2010).

4. Ocular responses to IOP-generated stress

Among the issues that will be considered next are whether the mechanisms by which the eye responds to IOP act immediately or require longer-term detection or response. Sensation mechanisms have timescales and sensitivities that allow the cell and tissue to function as band-pass filters, with some mechanisms quickly reacting to rapid fluctuation in stress and others that ignore quick variation and only are activated with continued change or particular levels of change. Some reviews distinguish sequential steps as 1) mechanosensation, 2) mechanoresponse, and 3) mechanotransmission (Hoffman et al., 2011). Mechanosensation includes elements such as bending of a cell membrane to open ionic channels or physical stress altering integrin-linked signaling at the membrane. Mechanoresponse mechanisms are implemented by various events, such as ion channel opening, collagen/elastin uncrimping, internal skeletal element unmasking of binding sites, cytokine release, and recruitment of integrins to signaling complexes. Mechanotransmission involves such long term processes such as transcription factor stimulation, reorganization of actin and intermediate filaments, cell process reorientation, and cell division.

The molecular and cellular processes that create band-pass filters thus allowing the precise interpretation of specific mechanical signals, while eliminating mechanical noise, are complex and incompletely understood. Cells detect mechanical stimuli through cell membrane mechanoreceptors, adherens junctions, cell-cell adhesions and junctions, integrin complexes, focal adhesions (FA), and primary cilia (Eyckmans et al., 2011; Leiphart et al., 2019; Martino et al., 2018). They respond to mechanical stimuli by activating intracellular

signaling pathways, activation of nuclear membrane complexes, cytoskeletal remodeling, changes in organelle morphology, and altered gene transcription. Cells are additionally active participants in probing their surroundings for mechanical cues. Band-pass filtering occurs on multiple levels including single proteins that can tune out mechanical cues, large protein complexes such as the cytoskeletal rearrangements, and cell-to-cell communication through direct cell contact or release of extracellular signals (Tapia-Rojo et al., 2020). The challenge to better understand glaucoma pathogenesis is to link our growing knowledge of IOP variation on multiple timescales and its role in glaucoma pathogenesis to the molecular responses to these stimuli.

In disease-oriented research, stress is often placed on the question of what pathological events initiate a decline in normal function. Instead, it may be more productive to consider that disease is a failure to maintain an equilibrium of forces that balance survival and detrimental mechanisms. Both beneficial and pathological pathways were activated in rat experimental glaucoma (Yang et al., 2007b). In animal glaucoma models, we produce an effect by an artificial stimulus; e.g., blocking aqueous humor outflow or crushing the optic nerve. In this setting, there is an exact starting point to gauge what are initial events. In chronic human glaucoma, on the other hand, the tissues exist in an ongoing milieu that produces either restoration of normal function or leads to loss of neurons. This precludes the ability to determine factors that might be considered “first” causes or earliest events. As we consider experimental data in the next sections, it is important to remember this difference between experimental artificiality and complex human disease. We will provide separate discussions of the individual tissues and cells of the ONH region that are relevant to IOP-produced stress.

4.1. Connective tissue responses of the optic nerve head

The ONH contains connective tissue primarily consisting of collagens and elastin, in both the LC and surrounding peripapillary sclera (PPS) (Fig. 2). As the main load-bearing component of the ONH, the primary function of this connective tissue is to resist the deformation response to IOP-generated stress (Quigley, 2015). Biomechanical modeling studies point to the LC and PPS as regions of greatest strain under the influence of IOP (Coudrillier et al., 2012; Grytz et al., 2012a; Norman et al., 2011). In an *ex vivo* inflation test on *post-mortem* human eyes, the maximum principal strain, E_{max}, which denotes the maximum tensile strain, measured using digital volume correlation (DVC) in the LC and PPS was approximately 3% when the eyes were subjected to controlled pressurization from 5 to 45 mmHg. Notably, the peripheral LC exhibited higher strain levels compared to the central LC and inner PPS, while the nasal quadrant showed lowest strain in both tissues (Midgett et al., 2020b). *In vivo* biomechanical studies conducted using OCT imaging to measure LC strains following acute IOP change in open angle glaucoma eyes have reported an average E_{max}, between 1 and 2% depending on the magnitude and percentage of IOP change (Czerpak et al., 2023a; Midgett et al., 2019), time from IOP change, and glaucoma stage (Czerpak et al., 2023a). A similar *in vivo* biomechanical study reported that the average effective strain of normal eyes, which is a measure of local shape distortion, ranged around 6.8%, and is higher than that measured in ocular hypertensive eyes (3.96%), primary open-angle glaucoma eyes (6.04%) and primary angle-closure glaucoma eyes (4.05%)

(Beotra et al., 2018). The LC, characterized by a fenestrated architecture with connective tissue beams, is recognized as a vulnerable spot within the eye, making it the primary site of injury in the case of glaucoma. It covers the opening of the scleral canal and tethers to the comparatively rigid PPS (Downs et al., 2010). In terms of connective tissue organization, the collagen and elastin fibrils of the LC in both human and monkey eyes are oriented directly across the ONH canal from one side to the other (Hernandez et al., 1987; Quigley, 2015). The PPS connective tissues are arranged in circumferential fashion around the ONH with interdigitations to LC beams. The other portion of the sclera to have this circumferential pattern is at the corneoscleral limbus. By contrast, the connective tissue of remainder of the sclera is primarily composed of types I and III collagen with no elastin, which are arranged in fibril groups called lamellae. Within each lamella, the collagen fibers are aligned in a dominant direction, while in adjacent lamellae, they alternate their orientations, ranging from anteroposterior to circumferential to oblique. The arrangement of the lamellae in the sclera resembled the interlacing pattern of a woven basket, with some degree of interweaving between them (Fig. 3) (Cone-Kimball et al., 2013). By contrast, in the PPS around the ONH, the woven basket arrangement changes to a circumferential pattern for both collagen and elastin fibrils in human (Hernandez et al., 1987; Quigley et al., 1991a) and in rodent eyes, (Gelman et al., 2010; Girard et al., 2011) which is seemingly designed to withstand hoop stress from IOP increase. In addition, the fiber diameter of collagen is larger in PPS (Quigley et al., 1991b) and the variance of fiber diameter is greater in PPS than LC where there is a relatively uniform collagen fiber (Anderson, 1969).

Connective tissue beams in the LC provide structural support to the RGC axonal bundles as they pass from the higher pressure of the posterior eye to the lower pressure myelinated optic nerve (Burgoyne et al., 2005; Downs et al., 2008). While in most eyes IOP-generated stress does not exceed the elastic limit of the LC beams, higher IOP has been shown to lead to extensive remodeling of the connective tissue structure, resulting in increased posterior displacement of the LC in glaucoma eyes (Burgoyne et al., 2005; Downs et al., 2008; Jonas et al., 2004; Quigley and Green, 1979; Ren et al., 2009). LC beams are thinner and occupy a lower proportion of the tissue in the superior and inferior poles of the ONH, and it is in these areas that initial glaucoma damage to axons is greatest (Emery et al., 1974; Ling et al., 2019; Quigley and Addicks, 1981; Radius et al., 1978). Previously mentioned biomechanical strain measurements in *postmortem* human eyes align with these findings, confirming that these polar areas have greater strain with induced IOP increase (Midgett et al., 2020a, 2020b). Both these studies and OCT imaging in living human eyes show that glaucoma and normal eyes differ in LC strains, with greater strains in glaucoma eyes with more damage at the time of testing (Czerpak et al., 2023a). Similarly, in mouse models of glaucoma, increased strains have been observed in astrocytic lamina (AL) in glaucoma groups induced through microbead injection or by treatment with recombinant trypsin enzyme (Korneva et al., 2020, 2022), as demonstrated in our previous biomechanical studies on the mouse ONH. Compatible with these findings, quantitative histological studies show that eyes with worse glaucoma damage have more curved LC (Czerpak et al., 2023b; Guan et al., 2022; Quigley et al., 1983) and thinner LC beams. Since these studies were cross-sectional in nature, they cannot differentiate between two possibilities: 1) eyes with greater strain at baseline become more damaged, or 2) as damage becomes greater, strain increases. Clearly,

remodeling of the ONH is likely to occur over time, performed by the actions of resident astrocytes and fibroblasts (Downs et al., 2011b; Yang et al., 2017). Roberts et al. have shown in a monkey model with early experimental glaucoma that the volume of the LC connective tissues initially increased in glaucomatous eyes compared to controls, by recruitment of more posterior beams (Roberts et al., 2009). Wang et al. examined 3D microstructure of human LC using OCT and observed that there is increased beam thickness to pore diameter ratios and higher pore diameter standard deviations in the glaucoma group, supporting the concept of remodeling during glaucoma progression (Wang et al., 2013). In addition, our recent microstructural study of human LC revealed that both mild and severe glaucoma eyes exhibit smaller pore diameter, greater beam tortuosity, and more isotropic beam structure compared to controls (Guan et al., 2022). Notably, studies conducted in a glaucomatous monkey model observed an increase in the production of type I, III, and IV collagen in LC (Morrison et al., 1990; Quigley, 2015). Furthermore, increase in collagen fiber mass in LC caused by IOP elevation was predicted using growth and remodeling framework in human glaucoma progression (Grytz et al., 2012b). These findings suggest that the augmented collagen production may serve to fill the former position of RGC axons in the lamina pores, but its organization would not likely serve the function of resisting mechanical strain as did the original beams. Brazile et al. reported that the tortuosity of collagen fibers diminished in thin LC beams which may allow the thinner beams to withstand similar amounts of IOP-induced force as thicker beams, despite the differences in beam width (Brazile et al., 2018). Alteration in collagen fiber crimp may enable the maintenance of a homeostatic strain condition without requiring changes in the diameter of the LC beams (Brazile et al., 2018; Grytz et al., 2020). Overall, the continuous remodeling process of connective tissue establishes a feedback mechanism with the mechanical behavior of LC, leading to a gradual reshaping of LC into a cup-like structure. Additionally, this reciprocal interaction between connective tissue remodeling and feedback mechanism contributes to the gradual posterior migration of the LC insertion site into the pia mater during the early stages of glaucoma (Downs et al., 2011b; Yang et al., 2011). As glaucomatous damage progresses with persistent connective tissue remodeling, the LC eventually becomes thinner to present the featured cupped, excavated morphology at the end stage of glaucoma (Downs et al., 2011b). In glaucoma, ongoing reorganization of connective tissue at LC defines the clinical picture of optic disc excavation and cupping.

Similar to remodeling in LC, the connective tissue of the PPS undergoes an adaptation process in response to the loading conditions associated with IOP. PPS thickness in monkey is thicker in the superior, inferior, and temporal quadrants, and comparatively thinner in the nasal quadrant (Downs et al., 2002; Yang et al., 2007a). Both studies in experimental mouse glaucoma and human glaucoma eyes show that the circumferential fiber pattern in the PPS (Coudrillier et al., 2012, 2013; Grytz et al., 2011) becomes more disordered compared to normal controls (Pijanka et al., 2012, 2014). The strain response of the PPS of human glaucoma donor eyes was significantly stiffer than that of normal eyes. Similarly, the stiffness of the PPS of mouse glaucoma models (Nguyen et al., 2013b) and the equatorial sclera in a monkey glaucoma model was substantially stiffer than normal (Gottanka et al., 1997). It is likely that the local difference in structure in PPS compared to the remainder of the sclera would lead to regionally different remodeling. Fazio et al. measured non-PPS

sclera compliance and found that it differed in monkeys at varying IOP exposures (Fazio et al., 2019). Since the biomechanical behaviors of PPS and LC are interconnected, the local response and remodeling of both tissues is an important area for further study.

4.2. Retinal ganglion cell responses

While it is the RGC that ultimately dies from glaucoma, it is not clear that the IOP-related events leading to axon injury derive primarily from the RGC axon itself. In fact, both hoop stress from the PPS and the translaminar cribrosa pressure gradient may act on other elements, both cellular and extracellular, that lead to detrimental events in the axon. However, human and animal studies of glaucoma detected abnormalities in RGC axons at the LC. Most notably, both anterograde and retrograde axonal transport are interrupted at this location in mice, rat, monkey and human glaucoma (Crish et al., 2010; Minckler et al., 1978; Pease et al., 2000; Quigley and Addicks, 1980; Quigley et al., 1981; Salinas-Navarro et al., 2010).

There are several pathways by which RGC death is known to be initiated (Almasieh et al., 2012). The intracellular c-Jun N-terminal kinase (JNK) stress response pathway has been implicated from a variety of evidence. c-Jun is upregulated in RGCs and astrocytes in glaucoma models (Hashimoto et al., 2005; Levkovitch-Verbin et al., 2005) and RGCs in human glaucoma eyes (Tezel et al., 2003). siRNA-mediated knockdown of c-Jun resulted in RGC survival after optic nerve lesion (Lingor et al., 2005). A JNK inhibitor produced moderate RGC protection in an acute ocular hypertension model (Sun et al., 2011). Mice lacking both Jnk2 and Jnk3 had improved RGC survival after injury (Fernandes et al., 2012). Most definitively, kinases upstream of JNK were shown to carry the injury signal in glaucoma and axon injury (Welsbie et al., 2013). Secondly, the block in retrograde axonal transport at the LC leads to neurotrophin withdrawal and a consequent initiation of apoptosis (Martin et al., 2003). Third, dysfunction in axonal mitochondria has been proposed to play a role, given the higher energy requirement of unmyelinated fibers at the LC (Dai et al., 2011). In a monkey glaucoma model, there are indications of microtubular disruption at an early stage of injury (Fortune et al., 2015). Each of the above mechanisms seems to be a consequence of some intervening and earlier step(s) produced by IOP-generated stress.

RGC and their axons contain mechanosensitive membrane channels that can sense IOP variations. Mechanosensitive channels in the RGC membrane include TRPV1, which has been shown to contribute to RGC death with experimental IOP elevation, likely through Ca^{++} ion entry into the cell or axon (McGrady et al., 2020; Sappington et al., 2009). Another mechanosensitive channel, pannexin-1 (Kurtenbach et al., 2014), is present in RGCs and interacts with a variety of cell response pathways. The mechanosensitive channels, Piezo 1 & 2, transmitting Ca^{++}, have been identified in RGCs (Morozumi et al., 2020). Altered calcium ion concentrations have been associated with effects on calmodulin and calpain with further changes in multiple kinases, as well as altered mitochondrial movement along microtubules—a known effect in glaucoma (Kimball et al., 2018; Quigley et al., 1981). Additional mechanosensitive channels found in RGC include TREK and TRAAK K^{+} channels, but their downstream effects in the axon or RGC soma have not been linked to cell survival mechanisms (Hughes et al., 2017). The RGC soma and their axons at the

ONH experience different levels and state of strains (e.g. tension, compression, shear, etc). Strains produced by IOP change are substantially greater in the ONH than in the retina (Yuan et al., 2023). A modeling study based on findings in mouse ONH suggests that the mechanical strains in the axon compartments are substantially greater than strains in supportive astrocytes (Ling et al., 2020). Thus, it is likely that IOP-generated stress on RGCs occurs predominantly in the axons at the ONH rather than in retinal RGC soma.

There is substantial evidence that some types and sizes of RGCs are more susceptible to human and experimental glaucoma. It is clinically well-established in OAG that the foveal or midget RGCs survive in the central retina longer than RGCs of this or other types in the mid-retina. Some evidence from both *post-mortem* human glaucoma eyes and from experimental monkey glaucoma confirms that larger RGCs die first (Dandona et al., 1991; Quigley et al., 1987, 1988). It has been suggested that some apparently greater loss of larger RGCs is due to pre-mortem shrinkage of cell body and axon (Morgan, 2002). Identification of RGC subtypes has become more nuanced with over 40 different subtypes of RGCs now classified in mammals (Zhang et al., 2022). These subtypes differ in anatomical morphology, electrophysiologic function, transcriptional profiles, and susceptibility to IOP and axonal damage (Daniel et al., 2018, 2019; El-Danaf and Huberman, 2015; Feng et al., 2013). While RGC phenotypes in primate and rodent retinas may not be concordant, large αRGCs (particularly OFF-type) are also more susceptible (Ou et al., 2016). It will be of interest to determine if differences in mechanosensation or mechanotranslation underlie differential sensitivities to IOP elevation, or if other factors such as nutritional needs (see Section 4.4) are contributory. In human eyes, larger RGC axons passing through the upper and lower poles of the optic nerve head are killed selectively and the connective tissues supporting them in these areas undergo greater biomechanical strains (Glovinsky et al., 1991; Midgett et al., 2020b; Quigley et al., 1988, 1989).

4.3. Astrocyte responses

The origins of the cellular response to external mechanical stimuli lie within the crosstalk between extracellular matrix (ECM) and mechanosensitive signaling molecules that include transmembrane channels, junctional complexes (JC), integrin-linked focal adhesions, and intramembrane and cytoskeletal proteins that respond to external mechanical stimuli (Figs. 4 and 5). These signaling pathways act as a band-pass filter–ignoring some external stimuli, while other stimuli activate either beneficial or detrimental cellular responses. Here, we describe the ONH astrocyte response to mechanical strain and highlight its dependence on frequency, magnitude, and duration.

We and others have shown that ONH astrocytes respond quickly and dramatically to changes in IOP in both rodent and monkey glaucoma models (Korneva et al., 2020; Morrison et al., 1990; Quillen et al., 2020; Tehrani et al., 2019). Mechanically-induced increase in intracellular Ca^{++} concentrations has been demonstrated for cultured retinal and brain astrocytes (Ho et al., 2014; Ostrow et al., 2011), and channels found in mouse ONH astrocytes include TRPC1, TRPP1,2, TRPM7, and Piezo2 (Choi et al., 2015). Defined fluid shear stress on cultured brain astrocytes in a microfluidic chamber generated non-uniform forces in actinin varying with stimulus rise time (Maneshi et al., 2018). Shear pulses with

fast rise times (2 ms) produced immediate increases in actinin tension and intracellular Ca^{++} increase, while slow ramp stimuli produced little Ca^{++} response. Cells integrate the effects of induced stress, with 10 narrow sequential pulses (11.5 dyn/cm^2 and 10 ms wide) causing 4 times the Ca^{++} increase of one pulse with that amplitude, but 100 ms wide. Thus, mechanoresponse in astrocyte ionic channels is determined not only by the magnitude of stress, but by duration and rise time (Maneshi et al., 2015). Further, Piezo channels act as frequency filters at onset and continuation of repetitive stimuli, indicating they are poor discriminators and inefficient transducers of continuous high-frequency stimulations. Their response depends on intrinsic channel gating, as well as the number of stimulated channels (Lewis et al., 2017). Moreover, the reaction of mechanosensitive channels is interdependent with cytoskeletal integrity and is both time dependent and viscoelastic. In astrocytes, treatment with cytochalasin-D – a potent inhibitor of actin polymerization– eliminated force gradients and changed the intracellular location of Ca^{++} elevation. Piezo2-mediated Ca^{++} influx activates RhoA to control changes in the actin cytoskeleton and the orientation of FA, representing mechanotranslational responses (Kirschner et al., 2021; Pardo-Pastor et al., 2018; Segel et al., 2019). In trabecular meshwork cells, the activity of mechanosensitive TREK-1 channels interacts with cochlin to produce changes in cytoskeletal remodeling (Carreon et al., 2017). Astrocyte populations are heterogeneous with diverse morphologies, gene transcription profiles, and roles in homeostasis and disease pathology (Escartin et al., 2021). Studies in different astrocyte populations, however, do provide insight into the potential for mechanical band-pass filters, potentially in ONH astrocytes. Together, these studies not only describe complex mechanosensitive band-pass filters in astrocytes but also highlight their crosstalk with cytoskeletal organization and the internal state of each cell.

Critical to the relevance of cell culture research in biomechanics is the issue of whether cultured astrocytes represent their actual response *in situ*, attached by integrin-linked signaling to their basement membranes and thus to the connective tissue matrix of ONH beams and PPS (Friedrich et al., 2017). ATP release from the mechanosensitive channel pannexin 1 was induced in cultured ONH astrocytes exposed to 5% equibiaxial strain (at 0.3 Hz for 2 min) (Beckel et al., 2014). This mild degree of strain was below that calculated as the mean strain present in the LC with a rise in IOP to 50 mm Hg (Sigal and Ethier, 2009). Cyclical stress at this level was hypothesized to be consistent with that of the ocular pulse as observed in primate eyes with remote telemetry (Downs et al., 2011a). Whether these *in vitro* conditions accurately model *in vivo* strain has not been established, nor has the relation of strain magnitude to IOP level.

An additional means for mechanosensation and mechanoresponses are JCs – multiprotein complexes that provide adhesion and integrin linkages (Hoffman et al., 2011) between ONH astrocytes and their collagenous basement membrane (Quillen et al., 2020). The electron dense appearance of these JCs is only present in astrocyte cytoplasm facing their basement membrane, suggesting that the JC role is intimately related to mechanosensitivity (Fig. 4). JC densities are not present in many astrocytes throughout the central nervous system, because they do not interact with a collagenous basement membrane and therefore do not serve a role in mechanosensation of collagenous ECM stress (Aten et al., 2022; Lunde et al., 2015). This unique role for transmembrane signaling pathways in ONH astrocytes was

demonstrated in gene expression differences between astrocytes of the ONH that have JC and those of the myelinated optic nerve that do not have JC (Keuthan et al., 2023).

Integrins – transmembrane receptors that participate in cell-ECM adhesion and mechanosensation – play a major role in astrocyte mechanosensation. Proteomic, immunoblot and immunofluorescent study of sclera and ONH in mouse glaucoma showed that integrin-linked signaling and actin cytoskeletal molecules are upregulated with increased IOP (Oglesby et al., 2016). Integrin dimers in the membrane are variously bonded to ECM components, including collagens I, III and IV, laminin and fibronectin in both the PPS and in ONH connective tissue beams in larger mammals (Morrison, 2006). Integrins are recruited to electron dense complexes in ONH astrocytes to translate external stress to a series of molecules that link them to the actin/myosin cytoskeleton (Tehrani et al., 2019). Particular integrin α/β dimers have specific extracellular linkages and are coupled to different intracellular signaling cascades (Kapp et al., 2017; Seetharaman and Etienne-Manneville, 2018). There are 24 known dimers of integrins, using 18 α and 8 β monomers. Whole mouse ONH tissue RNAseq data suggest a similar expression pattern of these dimer subunits: α2, 3, 5, V, 6 and 8 and β1 and 4. In normal monkey and human eyes, α2, α3, α6, β1, and β4 integrin subunits are localized in astrocytes along the margins of laminar beams and within glial columns (Morrison, 2006), which suggests that integrins $\alpha 2\beta 1$, $\alpha 3\beta 1$, $\alpha 6\beta 1$, and $\alpha 6\beta 4$ attach astrocytes to laminin in the basement membrane. Integrins α4, α5 and αv primarily label optic nerve head blood vessels, while α1, β2, and β3 were not found in monkey and human ONH tissue. In the core of LC beams in larger mammals and human eyes, there are no integrins identified, except associated with large and small blood vessels (Morrison, 2006).

Whether integrin binding is tension dependent is determined by the dimer and binding partner. α2β1 bound to collagen can withstand mechanical force >150 pN, whereas the fibronectin–α5β1 bond ruptures at 30–50 pN, and αVβ3 breaks at even lower forces (Niland et al., 2011). Integrins have a catch–slip bond, so applied force first strengthens the bond (the catch phase), but when force surpasses a threshold, the bond progressively weakens (slip regime) (Kechagia et al., 2019). Clustering of integrins into complexes induces “adhesion maturation” in which further force recruits additional integrins until, at a limit, the adhesion fails. This phenomenon could be the explanation of astrocyte separation from its basement membrane as observed in mouse experimental glaucoma (Dai et al., 2012; Lye-Barthel et al., 2013; Quillen et al., 2020) (Fig. 6).

The molecules linked to integrins include a variety of extracellular species, many secreted by the astrocytes themselves (Morrison, 2006). Integrins adhere to the astrocytic basement membrane, whose primary components are collagen IV, laminin, fibronectin, and glycosaminogly-cans. Data from the human protein database suggest that the most likely collagen IV trimer secreted by astrocytes is α5α5α6 (www.proteinatlas.org). Laminins form independent networks interdigitated with collagen IV and bind to cell membranes through the dystroglycan–glycoprotein complex. Laminins are composed of 3 non-identical chains: laminin α, β, and γ, forming a cruciform structure. There are five α, three β, and three γ chains, with 18 isoforms. Laminin-111 and −211 are astrocytic, while laminin-411 and −511 are endothelial and found in the basement membrane of brain microvessels (Kawauchi et al.,

2019). Analysis of the laminin—collagen IV complexes indicates that laminin binds to type IV collagen via the globular regions of either of its four arms (Charonis et al., 1985). The most likely the laminin trimers in astrocytes are: α1,4 or 5 with β2 and γ1.

The molecular response cascade internal to integrins (Hu et al., 2015) includes focal adhesion kinase (FAK), talin, vinculin, paxillin, zyxin and α-actinin, whose collective response alters the actin/myosin skeleton (Martino et al., 2018), through Rho and Rac-mediated (Konopka et al., 2016) interaction with paxillin, vinculin, and Src (Fig. 5) (Diniz et al., 2019). FAK is initially recruited to the integrin complex by paxillin and talin binding to integrins in response to external mechanical stimuli (Kleinschmidt and Schlaepfer, 2017) and its autophosphorylation activates downstream mechanotransducers (Martino et al., 2018). FAK activation increases paxillin phosphorylation, leading to a stronger cytoskeletal linkage, vinculin recruitment to adhesions, and focal adhesion maturation (Pasapera et al., 2010). The intrinsic mechano-signaling role of FAK involves Ras translocation to the nucleus (Zhou et al., 2015). Downstream signaling by force-mediated FAK activation triggers mechanosensitive cell proliferation and increased inflammatory cytokines (Wong et al., 2011). Short-term changes in some of these elements have been detected after acute IOP increase in rats (Tehrani et al., 2016), including acute decrease in FAK and increases in p-paxillin and p-cortactin. The interaction between FAK, talin and vinculin illustrates a mechanism whose effect on the actin cytoskeleton is calibrated by the force of mechanical stress, representing another band-pass filtering effect in the mechanoresponse (Rahikainen et al., 2019). Paxillin phosphorylated by FAK or Src binds activated vinculin, stabilizing FA-cytoskeleton interaction. Zyxin acts in mechanosensing by regulating F-actin polymerization (Uemura et al., 2011). The actin cytoskeleton is dynamic, so that high levels of α-actinin cross-linkage to the F-actin fibers indicate a resistant structure, while FAK phosphorylation of α-actinin leads to dissolution of the fiber linkage, as well as interacting with Rho activity on myosin—actin interaction to strengthen the fiber structure (Katsumi et al., 2004; Mitra et al., 2005). While much of the literature in the field deals with non-astrocytes, there is evidence that Bergmann glia – also known as radial astrocytes - have RhoA-mediated maintenance of F-actin fibers (Rosas-Hernandez et al., 2019). Rho kinase activity increases cell contractility and stiffness, while Rho kinase inhibition was neuroprotective in rat optic nerve crush (Yamamoto et al., 2014). Rho kinase inhibition in cultured human scleral fibroblasts and mouse glaucoma sclera decreases a-smooth muscle actin (α-SMA) increase and cell proliferation (Pitha et al., 2018).

The response of cells to their surrounding matrix is dependent upon its rigidity as well as changes in its stiffness (Hoffman et al., 2011). Models of this interaction suggest that on softer substrates or with slowly applied forces the FA molecular turnover is less than with rapidly applied force or stiffer matrices. A separate, but related mechanism involves inside—out signaling. Mechanical stress on the internal cytoskeleton leads not only to recruitment of actin to form cross-linked actin networks, but effects TGFβ release from its latent form in the extracellular matrix, stimulating its cell membrane receptor (Kirschner et al., 2021). Actin-based astrocyte structure and signaling within the ONH are significantly altered within hours after IOP elevation and prior to axonal cytoskeletal rearrangement, producing some responses that recover rapidly and others that persist for days despite IOP normalization (Wang et al., 2017). As described in the section on mechanosensitive

channels, this shows that the translational events caused by mechanical stress have time-dependent and time-limited, band-pass behaviors.

A separate intramembrane molecular complex sensitive to extracellular matrix behavior with intracellular signaling is the dystroglycan—glycoprotein complex (DGC). This consists of an extracellular α-dystroglycan and a membrane-spanning β subunit from a single gene product. DG binds to basement membrane components, especially laminins, as well as agrin and perlecan domains (Hohenester, 2019). DGC proteins consist of dystroglycan, α-dystrobrevin, and α-syntrophin. The complex is necessary for the localization of aquaporin 4 in the membrane. DG is a receptor for ECM laminin and agrin. While aquaporins are nearly ubiquitously found in brain astrocytes, they are absent in ONH astrocytes in all mammals, possibly to avoid swelling of astrocytes by aquaporin-dependent water intake in a structure that resists expansion (Kimball et al., 2022).

The cytoskeleton in astrocytes made up of F-actin and 10 nm intermediate filaments and few microtubules has both static micrometer scale stiffness and a turnover of its fibers that responds to other mechanical stimuli. The linkage of actin to myosin generates force changes. These protein—protein interactions have lifetimes that range from milliseconds to days (Evans and Calderwood, 2007), and applied force alters the life of non-covalent bonds, acting either as slip bonds or catch bonds (Thomas et al., 2008). Bonds between actin and the crosslinking protein α-actinin are slip bonds (Friedland et al., 2009), while the links between fibronectin and α5β1 integrin and actin–myosin act as catch bonds (Guo and Guilford, 2006). On longer time scales, cytoskeletal fibers can become reinforced or dissociated, changing the cellular internal structure (Leiphart et al., 2019). The balance between p-cofilin and cofilin in either stabilizing or dissociating the actin fibers is influenced by Rho kinase (Hayakawa et al., 2014), leading to transcriptional effects downstream in several signaling groups, including Wnt, Hippo and PI3K-Akt pathways. As indicated above, it is also influenced by mechanosensitive channel-induced change in Ca^{++} entry. Brain astrocytes express α-SMA under pathological conditions (Moreels et al., 2008; Pekny, 2001; Vedrenne et al., 2017). However, Clark et al. (Tovar-Vidales et al., 2016) found that cultured fibroblasts from human ONH beams expressed cross-linked actin networks, but cultured astrocytes did not. In DBA experimental or genetic glaucoma models in mice (Lye-Barthel et al., 2013; Wang et al., 2017), astrocyte processes thicken and alter position, suggesting dramatic changes in cytoskeleton. Astrocyte remodeling both precedes and is concomitant with glaucomatous axonal loss in DBA/2J mice (Bosco et al., 2016; Cooper et al., 2016, 2018). Cells align themselves in response to applied force, becoming parallel to static stretch, but becoming perpendicular to cyclic stretch (Faust et al., 2011; Prager-Khoutorsky et al., 2011). While this behavior has been studied in scleral fibroblasts in the eye (Szeto et al., 2021) and in both rat and mouse experimental glaucoma models, the ONH astrocytes reorient parallel to axons, aligning with the static IOP-generated stress (Quillen et al., 2020; Tehrani et al., 2014; Wang et al., 2017). In our recent study examining the cytoskeletal network in astrocytes within the mouse ONH, we observed regional differences in morphological changes in experimental glaucoma eyes 3 days after IOP elevation by bead injection, with significant variances in the unmyelinated ON regions. Specifically, the glaucoma group exhibited a significant increase in the measured areas of the ON, glial fibrillary acidic protein (GFAP), and actin within the unmyelinated ON regions. However,

the area fraction of GFAP decreased in the glaucoma group, whereas the area fraction of actin remained consistent between the two groups (Ling et al., 2020). We also observed in TEM of the astrocytic lamina 1–3 days after IOP elevation by bead injection, the appearance of abnormal extracellular spaces between astrocytes near the PPS, and of vesical and mitochondrial accumulation indicating axonal transport blockade. At 1 week, we also detected astrocytes separating from their basement membranes and new collagen formation (Quillen et al., 2020).

Intermediate filaments (IF) are found in 4 types, with type III typical for astrocytes, containing GFAP, vimentin and nestin. IFs form by self-assembly and have no molecular motors, such as myosin, associated with them (Etienne-Manneville, 2018). In astrocytes, dynamic IF polymerization and depolymerization is regulated by phosphorylation (Hol and Capetanaki, 2017), occurring over relatively longer timescales than for actin network alteration (Leduc and Etienne-Manneville, 2017). IFs are both more flexible and stretchable than actin and microtubules (Block et al., 2015). IFs are fully elastic, but at higher stress, they stiffen and decrease diameter (Herrmann and Aebi, 2016). Astrocytic type III IF association can be mediated by α and β synemins, which bind to talin, vinculin, zyxin, and α-actinin. Type III IF consist of mixtures of 10 GFAP isoforms (Moeton et al., 2016), vimentin, and nestin. GFAP is disassembled by calpain and S100α (Yang and Wang, 2015). The molecular mechanisms of dynamic association with junctional complexes by astrocytic, type III IFs include nestin- and integrin-mediated signaling through Rho GTPases. By atomic force microscopy, rat brain astrocytes increase in stiffness with age, due in part to changes in actin and IFs (Lee et al., 2015). IFs stabilize focal adhesions by binding to integrins, in some cases by associations linked by plectin and FAK (Nishimura et al., 2019) and focal adhesions are known to promote assembly of IF, suggesting a mutual interaction (Leube et al., 2015). It is likely that IFs serve as counter bearings for local actin–myosin forces.

In central nervous system astrocytes, GFAP labeling occupies only 15% of the astrocyte volume (Kacerovsky and Murai, 2016), but normal ONH astrocytes constitutively express GFAP, occupying a much larger proportion of astrocyte cytoplasm (Ling et al., 2020). In brain astrocytes, GFAP upregulates in response to injury (de Pablo et al., 2018; Guan et al., 2022). It could be concluded that the IOP-generated stress keeps ONH astrocytes in a constant state of response. In rat glaucoma models (Johnson et al., 2007; Morrison et al., 2005), GFAP was not increased over controls, contradicting *in vitro* studies of astrocytes placed under mechanical strain (Miller et al., 2009; Mulvihill et al., 2018). Fundamental differences between astrocytes *in situ* and in culture has now been identified as a serious problem in *in vitro* research that attempts to draw parallels with *in vivo* disease states.

Finally, astrocytes maintain constant intercellular communication with other astrocytes through connexin channels (Boal et al., 2021; Quigley, 1977a). This functional syncytium leads to coordinated responses over substantial distances that may extend to the fellow eye (Cooper et al., 2020; Nagy and Rash, 2000). Further cell-to-cell crosstalk involves mutual signaling with ONH microglia, as discussed below. Interestingly, rat glaucoma leads to a decrease in immunostaining for connexin 43 (Johnson et al., 2000), while in human glaucoma ONH, connexin 43 channels were reported to be increased in ONH and retina

(Kerr et al., 2011). Mechanical stress *in vitro* causes loss of connexin 43 based gap junctions in cultured ONH astrocytes (Hernandez et al., 2008), but again the relevance of cultured cells to their behavior *in situ* should be considered.

4.4. Capillary endothelium and pericytes

The zone of interaction between small blood vessels and neurons in the CNS is referred to as the neurovascular unit (Goncalves and Antonetti, 2022). In addition to capillary endothelial cells, the passage of molecules from the intravascular compartment is affected by pericytes, astrocytes, and microglia (Knopp et al., 2022). As described above, astrocytes in the ONH are interposed between capillaries and RGC axons. Pericytes occupy the connective tissue matrix between the capillary basement membrane and the astrocyte basement membrane, even in rodent ONH that lacks prominent connective tissue beams. Pericytes are more numerous in the retina and ONH than in the CNS capillaries in general (Frank et al., 1990). ONH capillaries are continuous with retinal and optic nerve capillaries and have tight junctions similar to CNS capillaries. Molecules that pass through the endothelial barrier must either be capable of transit through tight junctions or are carried by transcytoplasmic movement in caveolar vacuoles (Parton and del Pozo, 2013). Even molecules as small as fluorescein (molecular weight, 323) do not pass through the normal blood—ONH barrier. However, LC axons are exposed to some larger molecules leaking from choriocapillaries at the ONH periphery (Tso et al., 1975). There is no direct evidence that dysfunction in the blood—brain barrier at the ONH results from levels of IOP seen in OAG. There is no direct evidence that ONH capillaries actively constrict to manage flow.

The ONH is subject to mechanical stress produced by two forces: the circumferentially directed hoop stress of the PPS generated by IOP and the stress produced by the translaminar gradient between normally higher IOP and lower optic nerve tissue pressure (Morgan et al., 1998). In larger mammals, connective tissue beams based at the peripapillary sclera pass across the ONH, lined by astrocytes and containing within them capillaries and fibroblasts. Thus, LC capillaries, astrocytes, and axons are subject to biomechanical effects not seen in either retina or myelinated optic nerve, nor anywhere else in the brain. Capillaries express integrins within their luminal membrane, sensitive to both mechanical stress and shear, though the flow rates in small vessels do not likely produce high shear. Vascular endothelial cells are known to express integrins $\alpha 3\beta 1$, $\alpha 6\beta 1$, and $\alpha 6\beta 4$, $\alpha 5\beta 1$ and $\alpha v\beta 1$ (Morrison, 2006). Arteries have Piezo channels that can respond to shear (John et al., 2018) and their activation in arterial endothelium by disturbed flow leads to integrin activation of focal adhesion kinase-dependent NF-κB activity (Albarran-Juarez et al., 2018). It is postulated that compression in the LC is a cause of the clinical entity, central retinal vein occlusion (Green et al., 1981). Flow in retinal and ONH capillaries is autoregulated, maintaining normal flow up to IOP levels to 25 mm Hg below the mean arterial pressure (Quigley and Anderson, 1976; Quigley et al., 1985). Dysfunction in vascular autoregulation is implicated in the pathogenesis of some forms of glaucomatous optic neuropathy (Flammer and Konieczka, 2017). However, this is reported to occur in lower IOP phenotypes of OAG and may be relatively unrelated to IOP-produced stress. Lower blood pressure combined with higher IOP is epidemiologically associated with OAG, but there is, yet no method to quantify nutritional blood flow in living human eyes (Tielsch et al., 1995).

At the posterior LC border is the first node of Ranvier for RGC axons that are unmyelinated to that point. The high concentration of axonal mitochondria at this site has been hypothesized to indicate a high metabolic requirement needed for the generation of axonal non-saltatory transmission of action potentials (Minckler et al., 1976). Mitochondria move both anterograde and retrograde in axons, with evidence suggesting that damaged and aged mitochondria return to the RGC soma for “recharging” and axonal redistribution to maintain axonal health (Hung, 2021; Mandal et al., 2021). Their motion is reduced by IOP-generated stress at the ONH (Kimball et al., 2018).

The extracellular provision of energy-carrying metabolites to axons is now thought to include both glucose and lactate. This energy transfer begins with glucose exiting capillaries via the glucose transporter 1 (GLUT1) channel (also known as solute carrier family 2, facilitated glucose transporter member 1 (SLC2A1)) and entering the astrocyte through GLUT1 channels in their membrane (Carreras et al., 2015). The large stores of glycogen in astrocytes of the ONH indicate that much glucose is stored in that form. Through glycolysis, lactate is produced and passes out of the astrocytes through monocarboxylate transporter 1 (MCT1, also known as SLC16A1)) (Bergersen et al., 2002) and into the axon through their MCT2 channels (Pierre et al., 2000) in a process termed the astrocyte–neuron lactate shuttle (Pellerin et al., 1998). L-lactate derived from astrocyte glycogen has been shown to briefly sustain optic nerve axons (Tekkok et al., 2005). In the myelinated nerve, oligodendroglia support axons through MCTl-based transport of lactate and/or pyruvate (Lee et al., 2012). Interestingly, recent research in mouse glaucoma models suggests a neuroprotective effect of supplemental nicotinamide/pyruvate (Harder et al., 2020). While oxygen is clearly also supplied by capillaries to ONH axons, hyperbaric oxygenation was not protective from high IOP induced axon damage in monkeys (Quigley et al., 1980). Furthermore, blood flow is not quantitatively reduced in experimental monkey glaucoma (Quigley et al., 1985). Nor is the number of capillary profiles per unit tissue area reduced in monkey or human glaucoma (Quigley et al., 1984).

4.5. Microglia

While microglia occupy only a modest proportion of ONH cells, they actively respond in the glaucomatous retina (Hayreh et al., 1999; Kanamori et al., 2005; Lam et al., 2003; Wang et al., 2000). It has been demonstrated that microglia exhibit Piezo1 channels (Hu et al., 2023). Additionally, the mechanically and osmotically responsive ion channel, TRPV4, tunes the microglial inflammatory response to variations in matrix stiffness (Ayata and Schaefer, 2020). Furthermore, they show phenotypical and migratory responses to variations in matrix stiffness in brain (Ayata and Schaefer, 2020). However, some microglial changes could be due to known interactions between microglia and astrocytes rather than a direct mechanosensitive response from the microglia. In experimental glaucoma, both microglia and astrocytes proliferate (Kimball et al., 2021). The stimulation of astrocytes by microglia depends upon cytokines including complement 1q, interleukin 1b, and tumor necrosis factor α (Liddelow et al., 2017). A direct link between microglial activation and mechanical cues (alterations in tissue stiffness, microarchitecture, or mechanical strain) in glaucoma has not been established.

4.6. Fibroblasts of the lamina and PPS

The main cellular components of sclera stroma are fibroblasts and α-SMA-expressing myofibroblasts that are closely approximated to their surrounding ECM. In mouse eyes, fibroblasts are organized in cellular lamellae that are arranged between layers of collagenous fibrils with cellular lamellae comprising approximately 20% of the total thickness of fixed scleral tissue (Cone-Kimball et al., 2013). Ultrastructural studies revealed that fibroblasts have a polygonal morphology, long extensions, and points of contact between neighboring cells within and between cellular lamellae (Murata et al., 2019). Intercellular gap junctions, tight junctions, and intermediate junctions were seen in primate eyes which suggest that scleral fibroblasts could act as a cellular syncytium (Raviola et al., 1987). In human sclera, fibroblast actin filaments are highly aligned with surrounding collagen fibrils and actin filament organization varies in a manner that parallels regional differences in collagen organization (Fig. 7) (Szeto et al., 2021). In the peripheral sclera, actin and collagen fibrils are organized in a basket-weave pattern and in the PPS they are organized in concentric circles around the optic nerve head. The high degree of alignment is facilitated by the expression of integrins that enable cell-ECM attachment and FA formation (Hu et al., 2011; McBrien et al., 2006; Shelton and Rada, 2009). These contact points between scleral cells and their surrounding ECM, in turn, allow cells to react and respond to stimuli caused by IOP fluctuations.

Cultured scleral fibroblasts activate multiple signaling pathways and undergo cytoskeletal reorganization when placed under mechanical strain. When placed under static strain, primary scleral fibroblasts isolated from young donors undergo transcriptional changes in genes involved in ECM turnover, protein and lipid metabolism, and cell growth and differentiation (Cui et al., 2004). When primary fibroblasts from adult donors were placed under cyclic strain, cells similarly had changes in the transcription of genes involved in ECM synthesis and degradation, myofibroblast differentiation, inflammation, and activation of mechanoresponsive pathways such as the YAP and ROCK kinase signaling pathways (Hu et al., 2021; Qiu et al., 2022; Xie et al., 2020; Yamaoka et al., 2001; Yuan et al., 2018). Inhibition of YAP of ROCK signaling blunted the fibroblast response to mechanical strain and inhibited strain-induced myofibroblast differentiation. Transcriptional changes generated by cell strain are accompanied by alterations in cell migration, proliferation, and actin reorganization that vary depending on the degree of strain (Chagnon-Lessard et al., 2017; Neidlinger-Wilke et al., 2001; Szeto et al., 2021; Tamiello et al., 2015; Wang and Grood, 2000). Markov et al. showed that reversible strain-induced actin filament reorganization in bovine scleral fibroblasts was delayed when cells were placed under pathologic strain conditions compared to physiologic strain (Markov et al., 2022).

Fibroblast to myofibroblast differentiation can be influenced by tuning strain parameters from “physiologic” to “pathologic” levels. Qu et al. placed primary cultured human PPS fibroblasts under various cyclic strain conditions for 24 h and found that increased strain amounts (4% versus 1%) and higher strain frequency (5 Hz versus 0.5 or 0.05 Hz) induced proportionately more myofibroblast differentiation (Qu et al., 2015). This response, however, was not seen in all cell lines tested. While 7 of the 8 cell lines tested showed this pattern of response with the greatest myofibroblast differentiation induced under conditions

of high and rapid strain, one line had a paradoxical decrease in contractility when placed under 4% (pathologic) strain conditions. This cell line had a baseline myofibroblast content that was >3x higher than the other 7 cell lines which suggests that different fibroblast lineages could have variable responses to mechanical strain. Perhaps myofibroblasts respond to cyclic mechanical strain by decreasing contractile machinery while fibroblasts respond with an increase in contractility. In support of this hypothesis, Qiu et al. found differing responses to cyclic mechanical strain between cell lines isolated from the peripheral and peripapillary sclera (Qiu et al., 2018). Peripheral scleral fibroblasts placed under 10% strain (0.5 Hz) increased cell proliferation, α-SMA expression, and migratory rates while peripapillary scleral fibroblasts had an opposing response with reduced α-SMA expression and migration. Again, in these studies, the cell line with a paradoxical response (the PPS fibroblast cell line) had a much higher baseline level of α-SMA and a presumed higher myofibroblast content than the peripheral fibroblast cell line used. Further supporting the differential response of myofibroblasts to mechanical strain, PPS fibroblasts pretreated with myofibroblast-inducing levels of TGFβ and exposed to cyclic mechanical strain gained the ability to overcome topographic barriers that prevented migration of unstimulated fibroblasts (Szeto et al., 2021). These findings suggest that the fibroblast response to mechanical stimuli is not only gated with greater and more frequent strain causing a larger cellular response but that the nature of the response cannot be generalized across different fibroblast subtypes. It is therefore possible that one fibroblast subtype might have a physiologic or protective response to the strain conditions that cause a pathologic response in another subtype.

In vitro studies are facilitated by the relative ease with which scleral fibroblasts can be isolated and cultured from cadaveric donors. *In vitro* studies, however, have several notable limitations. It is not possible to recapitulate the complex extracellular environment, cell-cell interactions, and metabolic conditions that are present in scleral tissue. The kinetics, extent, and complex vectors of IOP-induced mechanical strain have not yet been modeled fully by *in vitro* methods. Therefore, strain experiments performed in cell culture do not fully model IOP-induced strain. Additionally, *in vitro* experiments are often conducted over 8–24 h. As cells transition from acute to prolonged strain durations, mechanoresponsive signaling pathways can change. During mitral valvulogenesis, acute strain induced RhoA-dominated signaling, while chronic strain led to a transition to Rac1-dependent signaling (rho Gould et al., 2016). Lastly, variables in isolation and culture techniques and donor characteristics could limit the generalizability of *in vitro* studies. To gain a more complete understanding of the fibroblast response to IOP-induced mechanical strain, *in vivo* studies are required.

Oglesby et al. performed proteomic analysis of mouse sclera after bead-induced (BI) IOP elevation (Oglesby et al., 2016). This method produces unilateral IOP elevation from a baseline of ~15 mmHg–~25 mmHg that is sustained for 1–3 weeks and is associated with scleral stiffening, collagen reorganization in the PPS, and quantifiable RGC loss at 6 weeks after bead injection. The cellular response to IOP elevation was rapid with increased cellular proliferation detected at 3 days that peaked at 7 days and persisted for 6 weeks. Along with proliferation, canonical integrin-linked, actin cytoskeleton and rho family GTPase pathway signaling was increased. There was significant αSMA induction indicating a transition to a more myofibroblast rich cellular environment following IOP elevation. This response was modifiable by targeting focal adhesion and cytoskeletal signaling using small molecule

inhibitors of rho-associated and src-kinase which prevented myofibroblast differentiation and reduced IOP-induced proliferation. Further, *in vivo* and *ex vivo* studies will be needed to understand better the role of IOP-induced mechanical strain in modifying scleral cellular activity and to determine if this response drives or antagonizes glaucoma progression.

In vivo studies in rodent models, however, have limitations due to anatomic differences between rodent and human eyes. Mouse and human PPS differ in several ways: (1) in mouse eyes, as sclera approaches the ONH, it splits to form connections to the meninges posteriorly and connection to the ONH in the peripapillary region, (2) the central retinal artery and vein run along the inferior border of the mouse optic nerve, while they are found centrally in human ONH, and (3) rodent eyes contain a vascular plexus that surrounds the optic nerve within the optic canal (Pazos et al., 2015, 2016). Aside from these differences and obvious differences in scale between rodent and human eyes, scleral structure is otherwise conserved between rodents in humans. Like human eyes, sclera is thickest in the PPS region and thinnest in the equatorial regions (Myers et al., 2010). In both human and rodent eyes, peripheral sclera contains collagen lamellae that are arranged in a basket weave pattern, while PPS collagen assumes an ordered circumferential orientation (Boote et al., 2019; Gelman et al., 2010). Importantly, human and mouse sclera remodel similarly in glaucoma. PPS in glaucomatous eyes is stiffer than age-matched normal sclera and PPS becomes less circumferentially aligned (Nguyen et al., 2013a; Pijanka et al., 2015). Additionally, the structural role of the PPS in translating IOP stress to the ONH has been demonstrated in both rodent and human eyes.

The fibroblast response to changes in scleral tissue stiffness that occur in glaucoma and with aging is currently unknown. Fibroblasts respond to substrates of varied stiffness by cytoskeletal and migratory changes, changes in gene transcription, and increased myofibroblast content occurs as tissue stiffens. However, the work describing this effect utilized tunable substrates that span stiffnesses that start at 1–5 kPa and usually peaked at ~50 kPa (Balestrini et al., 2012; Discher et al., 2005; Emig et al., 2021; Godbout et al., 2013; Huang et al., 2012; Liu et al., 2015; Piersma et al., 2015; van Putten et al., 2016). Scleral stiffness is orders of magnitude greater at baseline and the degree of relative stiffening in glaucomatous eyes is much smaller (Boote et al., 2019; Coudrillier et al., 2012, 2015; Liu et al., 2018b). It is not known whether these relative changes in ECM stiffness impact scleral fibroblast behavior.

The LC is a specialized matrix that is maintained by a distinct population of cells called lamina cribrosa cells. LC cells are GFAP negative, polygonal in morphology, and are located between and within the cribiform plates of the LC (Hernandez et al., 1988). While they share some features with scleral cells, they are morphologically distinct from scleral fibroblasts (Hernandez et al., 1988). To date, LC cells have been studied as primary cultures from cadaveric normal and glaucomatous donors but have not been studied or imaged *in vivo*. While their response to a variety of different relevant stressors has been examined, such as mechanical stimuli and hypoxia (Kirwan et al., 2012), and oxidative stress (Irnaten et al., 2018, 2020b), we focus on their response to mechanical stimuli. When exposed to cyclic mechanical strain, LC cells undergo transcriptional changes in genes involved in ECM remodeling, fibrosis, and TGFβ signaling (Kirwan et al., 2004; Quill et al., 2011).

ECM remodeling and TGFβ-signaling transcripts were differentially regulated in low (3%) versus high (20%) intensity strain conditions. This response was non-linear as there was only 1 differentially regulated transcript when comparing 3% versus 12% strain, but 15 differentially regulated transcripts when 3% was compared to 20% strain (Quill et al., 2011). Exposure to hypotonic solution causes cell swelling and has been used as a model of cell stretch. When exposed to hypotonic conditions, LC cells activated stretch-activated ion channels, increased intracellular Ca^{++}, and activated PKCα, p38, and p42/p44-MAPK (Irnaten et al., 2009, 2013, 2018; Quill et al., 2015). LC cells responded to changes in substrate stiffness. Myofibroblast differentiation of LC cells was increased on stiff (100 kPa) versus soft (4 kPa) substrates. Activation of the mechanoresponsive YAP signaling pathway was increased on stiff substrates and YAP inhibition was sufficient to inhibit myofibroblast transdifferentiation (Liu et al., 2018a; Murphy et al., 2022).

LC cells from glaucomatous eyes adopt a profibrotic phenotype with altered expression of mechanoresponsive signaling molecules. Microarray analysis of LC cell lines isolated from normal and glaucomatous eyes found significant upregulation of myofibroblast markers, TGFβ-signaling molecules, and ECM genes in LC cells isolated from glaucomatous donors (Kirwan et al., 2009). Exposing LC cells from normal donors to glaucomatous stimuli such as TGFβ, hypoxia, oxidative stress, cell stretch, or increased tissue stiffness induced a myofibroblast phenotype that could drive LC remodeling in glaucoma (Irnaten and O'Brien, 2023; Liu et al., 2018a; Liu et al., 2018b; Murphy et al., 2022). LC cells from glaucomatous eyes have abnormal calcium signaling, mitochondrial dysfunction, increased markers of oxidative stress, increased glycolysis, and increased baseline proliferation compared to LC cells from normal eyes (Irnaten et al., 2013; Irnaten et al., 2020a; Irnaten and O'Brien, 2023; Irnaten et al., 2020b; Irnaten et al., 2018; Kamel et al., 2020; Murphy et al., 2022). These differences occur in parallel with altered expression in glaucomatous LC cells of mechanoresponsive ion channels and signaling proteins that include L-type Ca channels, Ca-dependent Maxi-K, stretch-activated cation channels TRPC1 and TRPC6, and YAP (Irnaten and O'Brien, 2023; Irnaten et al., 2020b; Irnaten et al., 2018; Murphy et al., 2022). Whether the glaucomatous LC cell phenotype is reactive and protective or pathologic in glaucomatous eyes has not been established.

5. Summary

Currently, IOP reduction is the only clinically proven approach to prevent glaucoma progression. Clinical decision making in glaucoma, however, is guided by an incomplete picture of IOP that does not account for regional IOP variations within the eye, second-to-second IOP changes, circadian IOP rhythms, or postural changes in IOP. Moreover, translation of IOP-induced mechanical stress though the eye is influenced by structural, material, and microarchitectural differences in functionally distinct regions of the eye that can be further amplified in glaucoma. Translation of IOP-stress ultimately affects cells that are tightly coupled to their surrounding ECM that, in turn, can remodel surrounding tissue or translate these stimuli to RGCs and neuro-inflammatory cells. The subcellular events that occur because of mechanical stress screen some stimuli – acting as a band-pass filter – while other stimuli elicit differing responses depending on the degree of strain, frequency of strain, ECM stiffness, cell type, and cell differentiation. A more complete understanding of

the interplay between IOP, the tissue response to IOP fluctuations, and the diverse cellular responses to IOP-induced mechanical strain is needed to understand which clinical IOP features are optimal therapeutic targets and how to stop the progression of glaucomatous vision loss.

Funding

This review did not receive any specific grant from funding agencies in the public, commercial, or not-for-profit sectors.

Data availability

No data was used for the research described in the article.

Abbreviations

α-SMA	alpha smooth muscle actin
AL	astrocytic lamina
BI	bead-induced
DGC	dystroglycan—glycoprotein complex
ECM	extracellular matrix
FA	focal adhesion
FAK	focal adhesion kinase
GFAP	glial fibrillary acidic protein
GLUT1	glucose transporter 1
IF	intermediate filaments
IOP	intraocular pressure
JC	junctional complexes
JNK	c-jun n-terminal kinase
LC	lamina cribrosa
MCT1	monocarboxylate transporter 1
mmHg	millimeters of mercury
OAG	open angle glaucoma
ONH	optic nerve head
PPS	peripapillary sclera
RGC	retinal ganglion cell

SLC2A1	solute carrier family 2, facilitated glucose transporter member 1
TGFβ	transforming growth factor - beta

References

Albarran-Juarez J, Iring A, Wang S, Joseph S, Grimm M, Strilic B, Wettschureck N, Althoff TF, Offermanns S, 2018. Piezo1 and G(q)/G(11) promote endothelial inflammation depending on flow pattern and integrin activation. J. Exp. Med 215, 2655–2672. [PubMed: 30194266]

Almasieh M, Wilson AM, Morquette B, Cueva Vargas JL, Di Polo A, 2012. The molecular basis of retinal ganglion cell death in glaucoma. Prog. Retin. Eye Res 31, 152–181. [PubMed: 22155051]

Anderson DR, 1969. Ultrastructure of human and monkey lamina cribrosa and optic nerve head. Arch. Ophthalmol 82.

Anderson DR, Hendrickson A, 1974. Effect of intraocular pressure on rapid axoplasmic transport in monkey optic nerve. Invest. Ophthalmol 13, 771–783. [PubMed: 4137635]

Aten S, Kiyoshi CM, Arzola EP, Patterson JA, Taylor AT, Du Y, Guiher AM, Philip M, Camacho EG, Mediratta D, Collins K, Boni K, Garcia SA, Kumar R, Drake AN, Hegazi A, Trank L, Benson E, Kidd G, Terman D, Zhou M, 2022. Ultrastructural view of astrocyte arborization, astrocyte-astrocyte and astrocyte-synapse contacts, intracellular vesicle-like structures, and mitochondrial network. Prog. Neurobiol 213, 102264. [PubMed: 35283239]

Ayata P, Schaefer A, 2020. Innate sensing of mechanical properties of brain tissue by microglia. Curr. Opin. Immunol 62, 123–130. [PubMed: 32058296]

Bagga H, Liu JH, Weinreb RN, 2009. Intraocular pressure measurements throughout the 24 h. Curr. Opin. Ophthalmol 20, 79–83. [PubMed: 19240539]

Balestrini JL, Chaudhry S, Sarrazy V, Koehler A, Hinz B, 2012. The mechanical memory of lung myofibroblasts. Integr. Biol 4, 410–421.

Barkan O, 1954. Narrow-angle glaucoma; pupillary block and the narrow-angle mechanism. Am. J. Ophthalmol 37, 332–350. [PubMed: 13138686]

Beckel JM, Argali AJ, Lim JC, Xia J, Lu W, Coffey EE, Macarak EJ, Shahidullah M, Delamere NA, Zode GS, Sheffield VC, Shestopalov VI, Laties AM, Mitchell CH, 2014. Mechanosensitive release of adenosine 5'-triphosphate through pannexin channels and mechanosensitive upregulation of pannexin channels in optic nerve head astrocytes: a mechanism for purinergic involvement in chronic strain. Glia 62, 1486–1501. [PubMed: 24839011]

Beotra MR, Wang X, Tun TA, Zhang L, Baskaran M, Aung T, Strouthidis NG, Girard MJA, 2018. In vivo three-dimensional lamina cribrosa strains in healthy, ocular hypertensive, and glaucoma eyes following acute intraocular pressure elevation. Invest. Ophthalmol. Vis. Sci 59, 260–272. [PubMed: 29340640]

Bergersen L, Rafiki A, Ottersen OP, 2002. Immunogold cytochemistry identifies specialized membrane domains for monocarboxylate transport in the central nervous system. Neurochem. Res 27, 89–96. [PubMed: 11926280]

Block J, Schroeder V, Pawelzyk P, Willenbacher N, Koster S, 2015. Physical properties of cytoplasmic intermediate filaments. Biochim. Biophys. Acta 1853, 3053–3064. [PubMed: 25975455]

Boal AM, Risner ML, Cooper ML, Wareham LK, Calkins DJ, 2021. Astrocyte networks as therapeutic targets in glaucomatous neurodegeneration. Cells 10.

Boote C, Si gal IA, Grytz R, Hua Y, Nguyen TD, Girard MJA, 2019. Scleral structure and biomechanics. Prog. Retin. Eye Res, 100773 [PubMed: 31412277]

Bosco A, Breen KT, Anderson SR, Steele MR, Calkins DJ, Vetter ML, 2016. Glial coverage in the optic nerve expands in proportion to optic axon loss in chronic mouse glaucoma. Exp. Eye Res 150, 34–43. [PubMed: 26851485]

Brandt JD, 2004. Corneal thickness in glaucoma screening, diagnosis, and management. Curr. Opin. Ophthalmol 15, 85–89. [PubMed: 15021216]

Brazile BL, Hua Y, Jan NJ, Wallace J, Gogola A, Sigal IA, 2018. Thin lamina cribrosa beams have different collagen microstructure than thick beams. Invest. Ophthalmol. Vis. Sci 59.

Brubaker RF, 1991. Flow of aqueous humor in humans [The Friedenwald Lecture]. Invest. Ophthalmol. Vis. Sci 32, 3145–3166. [PubMed: 1748546]

Burgoyne CF, Downs JC, Bellezza AJ, Suh JK, Hart RT, 2005. The optic nerve head as a biomechanical structure: a new paradigm for understanding the role of IOP-related stress and strain in the pathophysiology of glaucomatous optic nerve head damage. Prog. Retin. Eye Res 24, 39–73. [PubMed: 15555526]

Bussel II, Wollstein G, Schuman JS, 2014. For glaucoma diagnosis, screening and detection of glaucoma progression. Br. J. Ophthalmol 98 (Suppl 2), ii15–19. [PubMed: 24357497]

Camras CB, Wax MB, Ritch R, Weinreb R, Robin AL, Higginbotham EJ, Lustgarten J, Stewart WC, Sherwood M, Krupin T, Wilensky J, Cioffi GA, Katz LJ, Schumer RA, Kaufman PL, Minckler D, Zimmerman T, Stjernschantz J, 1998. Latanoprost treatment for glaucoma: effects of treating for 1 year and of switching from timolol. United States Latanoprost Study Group. Am. J. Ophthalmol 126, 390–399. [PubMed: 9744372]

Carreon TA, Castellanos A, Gasull X, Bhattacharya SK, 2017. Interaction of cochlin and mechanosensitive channel TREK-1 in trabecular meshwork cells influences the regulation of intraocular pressure. Sci. Rep 7, 452. [PubMed: 28352076]

Carreras FJ, Aranda CJ, Porcel D, Rodriguez-Hurtado F, Martinez-Agustin O, Zarzuelo A, 2015. Expression of glucose transporters in the prelaminar region of the optic-nerve head of the pig as determined by immunolabeling and tissue culture. PLoS One 10, e0128516. [PubMed: 26030125]

Chagnon-Lessard S, Jean-Ruel H, Godin M, Pelling AE, 2017. Cellular orientation is guided by strain gradients. Integr. Biol 9, 607–618.

Charonis AS, Tsilibary EC, Yurchenco PD, Furthmayr H, 1985. Binding of laminin to type IV collagen: a morphological study. J. Cell Biol 100, 1848–1853. [PubMed: 3997977]

Choi HJ, Sun D, Jakobs TC, 2015. Astrocytes in the optic nerve head express putative mechanosensitive channels. Mol. Vis 21, 749–766. [PubMed: 26236150]

Cone-Kimball E, Nguyen C, Oglesby EN, Pease ME, Steinhart MR, Quigley HA, 2013. Scleral structural alterations associated with chronic experimental intraocular pressure elevation in mice. Mol. Vis 19, 2023–2039. [PubMed: 24146537]

Cooper ML, Collyer JW, Calkins DJ, 2018. Astrocyte remodeling without gliosis precedes optic nerve Axonopathy. Acta Neuropathol Commun 6, 38. [PubMed: 29747701]

Cooper ML, Crish SD, Inman DM, Horner PJ, Calkins DJ, 2016. Early astrocyte redistribution in the optic nerve precedes axonopathy in the DBA/2J mouse model of glaucoma. Exp. Eye Res 150, 22–33. [PubMed: 26646560]

Cooper ML, Pasini S, Lambert WS, D'Alessandro KB, Yao V, Risner ML, Calkins DJ, 2020. Redistribution of metabolic resources through astrocyte networks mitigates neurodegenerative stress. Proc. Natl. Acad. Sci. U.S.A 117, 18810–18821. [PubMed: 32690710]

Coudrillier B, Boote C, Quigley HA, Nguyen TD, 2013. Scleral anisotropy and its effects on the mechanical response of the optic nerve head. Biomech. Model. Mechanobiol 12, 941–963. [PubMed: 23188256]

Coudrillier B, Pijanka JK, Jefferys JL, Goel A, Quigley HA, Boote C, Nguyen TD, 2015. Glaucoma-related changes in the mechanical properties and collagen micro-architecture of the human sclera. PLoS One 10, e0131396. [PubMed: 26161963]

Coudrillier B, Tian J, Alexander S, Myers KM, Quigley HA, Nguyen TD, 2012. Biomechanics of the human posterior sclera: age- and glaucoma-related changes measured using inflation testing. Invest. Ophthalmol. Vis. Sci 53, 1714–1728. [PubMed: 22395883]

Crish SD, Sappington RM, Inman DM, Horner PJ, Calkins DJ, 2010. Distal axonopathy with structural persistence in glaucomatous neurodegeneration. Proc. Natl. Acad. Sci. U.S.A 107, 5196–5201. [PubMed: 20194762]

Cui W, Bryant MR, Sweet PM, McDonnell PJ, 2004. Changes in gene expression in response to mechanical strain in human scleral fibroblasts. Exp. Eye Res 78, 275–284. [PubMed: 14729359]

Curran EJ, 1920. A new operation for glaucoma involving a new principle in the aetiology and treatment of chronic primary glaucoma. Arch. Ophthalmol 49, 131–155.

Czerpak CA, Kashaf MS, Zimmerman BK, Quigley HA, Nguyen TD, 2023a. The strain response to intraocular pressure decrease in the lamina cribrosa of patients with glaucoma. Ophthalmol. Glaucoma 6.

Czerpak CA, Ling YTT, Jefferys JL, Quigley HA, Nguyen TD, 2023b. The curvature, collagen network structure, and their relationship to the pressure-induced strain response of the human lamina cribrosa in normal and glaucoma eyes. J. Biomech. Eng 1–33.

Dai C, Khaw PT, Yin ZQ, Li D, Raisman G, Li Y, 2012. Structural basis of glaucoma: the fortified astrocytes of the optic nerve head are the target of raised intraocular pressure. Glia 60, 13–28. [PubMed: 21948238]

Dai Y, Weinreb RN, Kim KY, Nguyen D, Park S, Sun X, Lindsey JD, Ellisman MH, Ju WK, 2011. Inducible nitric oxide synthase-mediated alteration of mitochondrial OPA1 expression in ocular hypertensive rats. Invest. Ophthalmol. Vis. Sci 52, 2468–2476. [PubMed: 21220562]

Dandona L, Hendrickson A, Quigley HA, 1991. Selective effects of experimental glaucoma on axonal transport by retinal ganglion cells to the dorsal lateral geniculate nucleus. Invest. Ophthalmol. Vis. Sci 32, 1593–1599. [PubMed: 1707861]

Danesh-Meyer HV, Boland MV, Savino PJ, Miller NR, Subramanian PS, Girkin CA, Quigley HA, 2010. Optic disc morphology in open-angle glaucoma compared with anterior ischemic optic neuropathies. Invest. Ophthalmol. Vis. Sci 51, 2003–2010. [PubMed: 19737875]

Daniel S, Clark AF, McDowell CM, 2018. Subtype-specific response of retinal ganglion cells to optic nerve crush. Cell Death Dis. 4, 7.

Daniel S, Meyer KJ, Clark AF, Anderson MG, McDowell CM, 2019. Effect of ocular hypertension on the pattern of retinal ganglion cell subtype loss in a mouse model of early-onset glaucoma. Exp. Eye Res 185, 107703. [PubMed: 31211954]

De Moraes CG, Mansouri K, Liebmann JM, Ritch R, Triggerfish C, 2018. Association between 24-hour intraocular pressure monitored with contact lens sensor and visual field progression in older adults with glaucoma. JAMA Ophthalmol 136, 779–785. [PubMed: 29800011]

de Pablo Y, Chen M, Mollerstrom E, Pekna M, Pekny M, 2018. Drugs targeting intermediate filaments can improve neurosupportive properties of astrocytes. Brain Res. Bull 136, 130–138. [PubMed: 28159699]

Diniz LP, Matias I, Siqueira M, Stipursky J, Gomes FCA, 2019. Astrocytes and the TGF-beta1 pathway in the healthy and diseased brain: a double-edged sword. Mol. Neurobiol 56, 4653–4679. [PubMed: 30377983]

Discher DE, Janmey P, Wang YL, 2005. Tissue cells feel and respond to the stiffness of their substrate. Science 310, 1139–1143. [PubMed: 16293750]

Downs JC, 2015. IOP telemetry in the nonhuman primate. Exp. Eye Res 141, 91–98. [PubMed: 26216571]

Downs JC, Blidner RA, Bellezza AJ, Thompson HW, Hart RT, Burgoyne CF, 2002. Peripapillary scleral thickness in perfusion-fixed normal monkey eyes. Invest. Ophthalmol. Vis. Sci 43.

Downs JC, Burgoyne CF, Seigfreid WP, Reynaud JF, Strouthidis NG, Sallee V, 2011a. 24-hour IOP telemetry in the nonhuman primate: implant system performance and initial characterization of IOP at multiple timescales. Invest. Ophthalmol. Vis. Sci 52, 7365–7375. [PubMed: 21791586]

Downs JC, Roberts MD, Burgoyne CF, 2008. Mechanical Environment of the Optic Nerve Head in Glaucoma.

Downs JC, Roberts MD, Burgoyne CF, 2010. Biomechanics of the Optic Nerve Head.

Downs JC, Roberts MD, Sigal IA, 2011b. Glaucomatous cupping of the lamina cribrosa: a review of the evidence for active progressive remodeling as a mechanism. Exp. Eye Res 93, 133–140. [PubMed: 20708001]

Drance SM, 1972. Some factors in the production of low tension glaucoma. Br. J. Ophthalmol 56, 229–242. [PubMed: 5032759]

El-Danaf RN, Huberman AD, 2015. Characteristic patterns of dendritic remodeling in early-stage glaucoma: evidence from genetically identified retinal ganglion cell types. J. Neurosci 35, 2329–2343. [PubMed: 25673829]

Elkington AR, Inman CB, Steart PV, Weller RO, 1990. The structure of the lamina cribrosa of the human eye: an immunocytochemical and electron microscopical study. Eye (Lond) 4 (Pt 1), 42–57. [PubMed: 2182351]

Emery JM, Landis D, Paton D, Boniuk M, Craig JM, 1974. The lamina cribrosa in normal and glaucomatous human eyes. Trans. Am. Acad. Ophthalmol. Otolaryngol 78, OP290–297. [PubMed: 4825057]

Emi K, Pederson JE, Toris CB, 1989. Hydrostatic pressure of the suprachoroidal space. Invest. Ophthalmol. Vis. Sci 30, 233–238. [PubMed: 2914753]

Emig R, Knodt W, Krussig MJ, Zgierski-Johnston CM, Gorka O, Gross O, Kohl P, Ravens U, Peyronnet R, 2021. Piezo1 channels contribute to the regulation of human atrial fibroblast mechanical properties and matrix stiffness sensing. Cells 10.

Escartin C, Galea E, Lakatos A, O'Callaghan JP, Petzold GC, Serrano-Pozo A, Steinhauser C, Volterra A, Carmignoto G, Agarwal A, Allen NJ, Araque A, Barbeito L, Barzilai A, Bergles DE, Bonvento G, Butt AM, Chen WT, Cohen-Salmon M, Cunningham C, Deneen B, De Strooper B, Diaz-Castro B, Farina C, Freeman M, Gallo V, Goldman JE, Goldman SA, Gotz M, Gutierrez A, Haydon PG, Heiland DH, Hoi EM, Holt MG, lino M, Kastanenka KV, Kettenmann H, Khakh BS, Koizumi S, Lee CJ, Liddelow SA, MacVicar BA, Magistretti P, Messing A, Mishra A, Molofsky AV, Murai KK, Norris CM, Okada S, Oliet SHR, Oliveira JF, Panatier A, Parpura V, Pekna M, Pekny M, Pellerin L, Perea G, Perez-Nievas BG, Pfrieger FW, Poskanzer KE, Quintana FJ, Ransohoff RM, Riquelme-Perez M, Robel S, Rose CR, Rothstein JD, Rouach N, Rowitch DH, Semyanov A, Sirko S, Sontheimer H, Swanson RA, Vitorica J, Wanner IB, Wood LB, Wu J, Zheng B, Zimmer ER, Zorec R, Sofroniew MV, Verkhratsky A, 2021. Reactive astrocyte nomenclature, definitions, and future directions. Nat. Neurosci 24, 312–325. [PubMed: 33589835]

Etienne-Manneville S, 2018. Cytoplasmic intermediate filaments in cell biology. Annu. Rev. Cell Dev. Biol 34, 1–28. [PubMed: 30059630]

Evans EA, Calderwood DA, 2007. Forces and bond dynamics in cell adhesion. Science 316, 1148–1153. [PubMed: 17525329]

Eyckmans J, Boudou T, Yu X, Chen CS, 2011. A hitchhiker's guide to mechanobiology. Dev. Cell 21, 35–47. [PubMed: 21763607]

Faust U, Hampe N, Rubner W, Kirchgessner N, Safran S, Hoffmann B, Merkel R, 2011. Cyclic stress at mHz frequencies aligns fibroblasts in direction of zero strain. PLoS One 6, e28963. [PubMed: 22194961]

Fazio MA, Girard MJA, Lee W, Morris JS, Burgoyne CF, Crawford Downs J, 2019. The relationship between scleral strain change and differential cumulative intraocular pressure exposure in the nonhuman primate chronic ocular hypertension model. Invest. Ophthalmol. Vis. Sci 60.

Feng L, Zhao Y, Yoshida M, Chen H, Yang JF, Kim TS, Cang J, Troy JB, Liu X, 2013. Sustained ocular hypertension induces dendritic degeneration of mouse retinal ganglion cells that depends on cell type and location. Invest. Ophthalmol. Vis. Sci 54, 1106–1117. [PubMed: 23322576]

Fernandes KA, Harder JM, Fornarola LB, Freeman RS, Clark AF, Pang IH, John SW, Libby RT, 2012. JNK2 and JNK3 are major regulators of axonal injury-induced retinal ganglion cell death. Neurobiol. Dis 46, 393–401. [PubMed: 22353563]

Flammer J, Konieczka K, 2017. The discovery of the Flammer syndrome: a historical and personal perspective. EPMA J. 8, 75–97. [PubMed: 28725290]

Flatau A, Solano F, Idrees S, Jefferys JL, Volpe P, Damion C, Quigley HA, 2016. Measured changes in limbal strain during simulated sleep in face down position using an instrumented contact lens in healthy adults and adults with glaucoma. JAMA Ophthalmol 134, 375–382. [PubMed: 26795708]

Flatau A, Solano F, Jefferys JL, Damion C, Quigley HA, 2018. A protective eye shield reduces limbal strain and its variability during simulated sleep in adults with glaucoma. J. Glaucoma 27, 77–86. [PubMed: 29194205]

Fortune B, Cull G, Reynaud J, Wang L, Burgoyne CF, 2015. Relating retinal ganglion cell function and retinal nerve fiber layer (RNFL) retardance to progressive loss of RNFL thickness and optic nerve axons in experimental glaucoma. Invest. Ophthalmol. Vis. Sci 56, 3936–3944. [PubMed: 26087359]

Frank RN, Turczyn TJ, Das A, 1990. Pericyte coverage of retinal and cerebral capillaries. Invest. Ophthalmol. Vis. Sci 31, 999–1007. [PubMed: 2354923]

Friedenwald JS, Moses R, 1950. Modern refinements in tonometry. Doc. Ophthalmol 4, 335–362. [PubMed: 15427579]

Friedland JC, Lee MH, Boettiger D, 2009. Mechanically activated integrin switch controls alpha5beta1 function. Science 323, 642–644. [PubMed: 19179533]

Friedrich O, Schneidereit D, Nikolaev YA, Nikolova-Krstevski V, Schurmann S, Wirth-Hucking A, Merten AL, Fatkin D, Martinac B, 2017. Adding dimension to cellular mechanotransduction: advances in biomedical engineering of multiaxial cell-stretch systems and their application to cardiovascular biomechanics and mechano-signaling. Prog. Biophys. Mol. Biol 130, 170–191. [PubMed: 28647645]

Gardiner SK, Fortune B, Wang L, Downs JC, Burgoyne CF, 2012. Intraocular pressure magnitude and variability as predictors of rates of structural change in nonhuman primate experimental glaucoma. Exp. Eye Res 103, 1–8. [PubMed: 22960316]

Gelman S, Cone FE, Pease ME, Nguyen TD, Myers K, Quigley HA, 2010. The presence and distribution of elastin in the posterior and retrobulbar regions of the mouse eye. Exp. Eye Res 90, 210–215. [PubMed: 19853602]

Girard MJA, Dahlmann-Noor A, Rayapureddi S, Bechara JA, Bertin BME, Jones H, Albon J, Khaw PT, Ross Ethier C, 2011. Quantitative mapping of scleral fiber orientation in normal rat eyes. Invest. Ophthalmol. Vis. Sci 52.

Glovinsky Y, Quigley HA, Dunkelberger GR, 1991. Retinal ganglion cell loss is size dependent in experimental glaucoma. Invest. Ophthalmol. Vis. Sci 32, 484–491. [PubMed: 2001923]

Godbout C, Follonier Castella L, Smith EA, Talele N, Chow ML, Garonna A, Hinz B, 2013. The mechanical environment modulates intracellular calcium oscillation activities of myofibroblasts. PLoS One 8, e64560. [PubMed: 23691248]

Goldmann H, 1954. [A new applanation tonometer]. Bull. Mem. Soc. Fr. Ophtalmol 67, 474–477 discussion, 477-478. [PubMed: 13284610]

Goncalves A, Antonetti DA, 2022. Transgenic animal models to explore and modulate the blood brain and blood retinal barriers of the CNS. Fluids Barriers CNS 19, 86. [PubMed: 36320068]

Gottanka J, Flügel-Koch C, Martus P, Johnson DH, Lütjen-Drecoll E, 1997. Correlation of pseudoexfoliative material and optic nerve damage in pseudoexfoliation syndrome. Invest. Ophthalmol. Vis. Sci 38.

Green WR, Chan CC, Hutchins GM, Terry JM, 1981. Central retinal vein occlusion: a prospective histopathologic study of 29 eyes in 28 cases. Retina 1, 27–55. [PubMed: 15633406]

Grytz R, Girkin CA, Libertiaux V, Downs JC, 2012a. Perspectives on biomechanical growth and remodeling mechanisms in glaucoma. Mech. Res. Commun 42.

Grytz R, Meschke G, Jonas JB, 2011. The collagen fibril architecture in the lamina cribrosa and peripapillary sclera predicted by a computational remodeling approach. Biomech. Model. Mechanobiol 10, 371–382. [PubMed: 20628781]

Grytz R, Sigal IA, Ruberti JW, Meschke G, Crawford Downs J, 2012b. Lamina cribrosa thickening in early glaucoma predicted by a microstructure motivated growth and remodeling approach. Mech. Mater 44, 99–109. [PubMed: 22389541]

Grytz R, Yang H, Hua Y, Samuels BC, Sigal IA, 2020. Connective Tissue Remodeling in Myopia and its Potential Role in Increasing Risk of Glaucoma.

Guan C, Pease ME, Quillen S, Ling YTT, Li X, Kimball E, Johnson TV, Nguyen TD, Quigley HA, 2022. Quantitative microstructural analysis of cellular and tissue remodeling in human glaucoma optic nerve head. Invest. Ophthalmol. Vis. Sci 63, 18.

Guo B, Guilford WH, 2006. Mechanics of actomyosin bonds in different nucleotide states are tuned to muscle contraction. Proc. Natl. Acad. Sci. U.S.A 103, 9844–9849. [PubMed: 16785439]

Harder JM, Guymer C, Wood JPM, Daskalaki E, Chidlow G, Zhang C, Balasubramanian R, Cardozo BH, Foxworth NE, Deering KE, Ouellette TB, Montgomery C, Wheelock CE, Casson RJ, Williams PA, John SWM, 2020. Disturbed glucose and pyruvate metabolism in glaucoma with neuroprotection by pyruvate or rapamycin. Proc. Natl. Acad. Sci. U.S.A 117, 33619–33627. [PubMed: 33318177]

Harwerth RS, Wheat JL, Fredette MJ, Anderson DR, 2010. Linking structure and function in glaucoma. Prog. Retin. Eye Res 29, 249–271. [PubMed: 20226873]

Hashimoto K, Parker A, Malone P, Gabelt BT, Rasmussen C, Kaufman PS, Hernandez MR, 2005. Long-term activation of c-Fos and c-Jun in optic nerve head astrocytes in experimental ocular hypertension in monkeys and after exposure to elevated pressure in vitro. Brain Res. 1054, 103–115. [PubMed: 16081055]

Hayakawa K, Sakakibara S, Sokabe M, Tatsumi H, 2014. Single-molecule imaging and kinetic analysis of cooperative cofilin-actin filament interactions. Proc. Natl. Acad. Sci. U.S.A 111, 9810–9815. [PubMed: 24958883]

Hayreh SS, Pe'er J, Zimmerman MB, 1999. Morphologic changes in chronic high-pressure experimental glaucoma in rhesus monkeys. J. Glaucoma 8, 56–71. [PubMed: 10084276]

Heijl A, Buchholz P, Norrgren G, Bengtsson B, 2013. Rates of visual field progression in clinical glaucoma care. Acta Ophthalmol. 91, 406–412. [PubMed: 23066646]

Heijl A, Leske MC, Bengtsson B, Hyman L, Bengtsson B, Hussein M, Early Manifest Glaucoma Trial, G., 2002. Reduction of intraocular pressure and glaucoma progression: results from the Early Manifest Glaucoma Trial. Arch. Ophthalmol 120, 1268–1279. [PubMed: 12365904]

Hernandez MR, Igoe F, Neufeld AH, 1988. Cell culture of the human lamina cribrosa. Invest. Ophthalmol. Vis. Sci 29, 78–89. [PubMed: 3275593]

Hernandez MR, Luo XX, Igoe F, Neufeld AH, 1987. Extracellular matrix of the human lamina cribrosa. Am. J. Ophthalmol 104, 567–576. [PubMed: 3318474]

Hernandez MR, Miao H, Lukas T, 2008. Astrocytes in glaucomatous optic neuropathy. Prog. Brain Res 173, 353–373. [PubMed: 18929121]

Herrmann H, Aebi U, 2016. Intermediate filaments: structure and assembly. Cold Spring Harbor Perspect. Biol 8.

Ho KW, Lambert WS, Calkins DJ, 2014. Activation of the TRPV1 cation channel contributes to stress-induced astrocyte migration. Glia 62, 1435–1451. [PubMed: 24838827]

Hoffman BD, Grashoff C, Schwartz MA, 2011. Dynamic molecular processes mediate cellular mechanotransduction. Nature 475, 316–323. [PubMed: 21776077]

Hohenester E, 2019. Laminin G-like domains: dystroglycan-specific lectins. Curr. Opin. Struct. Biol 56, 56–63. [PubMed: 30530204]

Hol EM, Capetanaki Y, 2017. Type III intermediate filaments desmin, glial fibrillary acidic protein (GFAP), vimentin, and peripherin. Cold Spring Harbor Perspect. Biol 9.

Hollows FC, Graham PA, 1966. Intra-ocular pressure, glaucoma, and glaucoma suspects in a defined population. Br. J. Ophthalmol 50, 570–586. [PubMed: 5954089]

Howell GR, Libby RT, Jakobs TC, Smith RS, Phalan FC, Barter JW, Barbay JM, Marchant JK, Mahesh N, Porciatti V, Whitmore AV, Masland RH, John SW, 2007. Axons of retinal ganglion cells are insulted in the optic nerve early in DBA/2J glaucoma. J. Cell Biol 179, 1523–1537. [PubMed: 18158332]

Hu D, Jiang J, Ding B, Xue K, Sun X, Qian S, 2021. Mechanical strain regulates myofibroblast differentiation of human scleral fibroblasts by YAP. Front. Physiol 12, 712509. [PubMed: 34658907]

Hu J, Chen Q, Zhu H, Hou L, Liu W, Yang Q, Shen H, Chai G, Zhang B, Chen S, Cai Z, Wu C, Hong F, Li H, Chen S, Xiao N, Wang ZX, Zhang X, Wang B, Zhang L, Mo W, 2023. Microglial Piezo1 senses Abeta fibril stiffness to restrict Alzheimer's disease. Neuron 111, 15–29 e18. [PubMed: 36368316]

Hu S, Cui D, Yang X, Hu J, Wan W, Zeng J, 2011. The crucial role of collagenbinding integrins in maintaining the mechanical properties of human scleral fibroblasts-seeded collagen matrix. Mol. Vis 17, 1334–1342. [PubMed: 21647271]

Hu S, Tee YH, Kabla A, Zaidel-Bar R, Bershadsky A, Hersen P, 2015. Structured illumination microscopy reveals focal adhesions are composed of linear subunits. Cytoskeleton (Hoboken) 72, 235–245. [PubMed: 26012525]

Huang X, Yang N, Fiore VF, Barker TH, Sun Y, Morris SW, Ding Q, Thannickal VJ, Zhou Y, 2012. Matrix stiffness-induced myofibroblast differentiation is mediated by intrinsic mechanotransduction. Am. J. Respir. Cell Mol. Biol 47, 340–348. [PubMed: 22461426]

Hughes S, Foster RG, Peirson SN, Hankins MW, 2017. Expression and localisation of two-pore domain (K2P) background leak potassium ion channels in the mouse retina. Sci. Rep 7, 46085. [PubMed: 28443635]

Hung C, 2021. Importance of retrograde axonal transport in mitochondrial health and distribution. Cell Death Dis. 7, 106.

Irnaten M, Barry RC, Quill B, Clark AF, Harvey BJ, O'Brien CJ, 2009. Activation of stretch-activated channels and maxi-K+ channels by membrane stress of human lamina cribrosa cells. Invest. Ophthalmol. Vis. Sci 50, 194–202. [PubMed: 18775862]

Irnaten M, Barry RC, Wallace DM, Docherty NG, Quill B, Clark AF, O'Brien CJ, 2013. Elevated maxi-K(+) ion channel current in glaucomatous lamina cribrosa cells. Exp. Eye Res 115, 224–229. [PubMed: 23906962]

Irnaten M, Duff A, Clark A, O'Brien C, 2020a. Intra-cellular calcium signaling pathways (PKC, RAS/RAF/MAPK, PI3K) in lamina cribrosa cells in glaucoma. J. Clin. Med 10.

Irnaten M, O'Brien CJ, 2023. Calcium-signalling in human glaucoma lamina cribrosa myofibroblasts. Int. J. Mol. Sci 24.

Irnaten M, O'Malley G, Clark AF, O'Brien CJ, 2020b. Transient receptor potential channels TRPC1/TRPC6 regulate lamina cribrosa cell extracellular matrix gene transcription and proliferation. Exp. Eye Res 193, 107980. [PubMed: 32088241]

Irnaten M, Zhdanov A, Brennan D, Crotty T, Clark A, Papkovsky D, O'Brien C, 2018. Activation of the NFAT-calcium signaling pathway in human lamina cribrosa cells in glaucoma. Invest. Ophthalmol. Vis. Sci 59, 831–842. [PubMed: 29411011]

Iyer JV, Boland MV, Jefferys J, Quigley H, 2021. Defining glaucomatous optic neuropathy using objective criteria from structural and functional testing. Br. J. Ophthalmol 105, 789–793. [PubMed: 32699052]

Jasien JV, Turner DC, Girkin CA, Downs JC, 2019. Cyclic pattern of intraocular pressure (IOP) and transient IOP fluctuations in nonhuman primates measured with continuous wireless telemetry. Curr. Eye Res 44, 1244–1252. [PubMed: 31170817]

Jensen AD, Maumenee AE, 1973. Home tonometry. Am. J. Ophthalmol 76, 929–932. [PubMed: 4759854]

Jin Y, Wang X, Zhang L, Jonas JB, Aung T, Schmetterer L, Girard MJA, 2018. Modeling the origin of the ocular pulse and its impact on the optic nerve head. Invest. Ophthalmol. Vis. Sci 59, 3997–4010. [PubMed: 30098188]

John L, Ko NL, Gokin A, Gokina N, Mandala M, Osol G, 2018. The Piezo1 cation channel mediates uterine artery shear stress mechanotransduction and vasodilation during rat pregnancy. Am. J. Physiol. Heart Circ. Physiol 315, H1019–H1026. [PubMed: 30004235]

Johnson EC, Deppmeier LM, Wentzien SK, Hsu I, Morrison JC, 2000. Chronology of optic nerve head and retinal responses to elevated intraocular pressure. Invest. Ophthalmol. Vis. Sci 41, 431–442. [PubMed: 10670473]

Johnson EC, Jia L, Cepurna WO, Doser TA, Morrison JC, 2007. Global changes in optic nerve head gene expression after exposure to elevated intraocular pressure in a rat glaucoma model. Invest. Ophthalmol. Vis. Sci 48, 3161–3177. [PubMed: 17591886]

Jonas JB, Berenshtein E, Holbach L, 2004. Lamina cribrosa thickness and spatial relationships between intraocular space and cerebrospinal fluid space in highly myopic eyes. Invest. Ophthalmol. Vis. Sci 45.

Kacerovsky BJ, Murai KK, 2016. Stargazing: monitoring subcellular dynamics of brain astrocytes. Neuroscience 323, 84–95. [PubMed: 26162237]

Kamel K, O'Brien CJ, Zhdanov AV, Papkovsky DB, Clark AF, Stamer WD, Irnaten M, 2020. Reduced oxidative phosphorylation and increased glycolysis in human glaucoma lamina cribrosa cells. Invest. Ophthalmol. Vis. Sci 61, 4.

Kanamori A, Nakamura M, Nakanishi Y, Yamada Y, Negi A, 2005. Long-term glial reactivity in rat retinas ipsilateral and contralateral to experimental glaucoma. Exp. Eye Res 81, 48–56. [PubMed: 15978254]

Kapp TG, Rechenmacher F, Neubauer S, Maltsev OV, Cavalcanti-Adam EA, Zarka R, Reuning U, Notni J, Wester HJ, Mas-Moruno C, Spatz J, Geiger B, Kessler H, 2017. A comprehensive

evaluation of the activity and selectivity profile of ligands for RGD-binding integrins. Sci. Rep 7, 39805. [PubMed: 28074920]

Katsumi A, Orr AW, Tzima E, Schwartz MA, 2004. Integrins in mechanotransduction. J. Biol. Chem 279, 12001–12004. [PubMed: 14960578]

Kawauchi S, Horibe S, Sasaki N, Hirata KI, Rikitake Y, 2019. A novel in vitro co-culture model to examine contact formation between astrocytic processes and cerebral vessels. Exp. Cell Res 374, 333–341. [PubMed: 30553966]

Kechagia JZ, Ivaska J, Roca-Cusachs P, 2019. Integrins as biomechanical sensors of the microenvironment. Nat. Rev. Mol. Cell Biol 20, 457–473. [PubMed: 31182865]

Keeler R, Singh AD, Dua H, 2013. Richard banister 1570–1625. Father of British ophthalmology. Br. J. Ophthalmol 7–8.

Kendell KR, Quigley HA, Kerrigan LA, Pease ME, Quigley EN, 1995. Primary open-angle glaucoma is not associated with photoreceptor loss. Invest. Ophthalmol. Vis. Sci 36, 200–205. [PubMed: 7822147]

Kerr NM, Johnson CS, Green CR, Danesh-Meyer HV, 2011. Gap junction protein connexin43 (GJA1) in the human glaucomatous optic nerve head and retina. J. Clin. Neurosci 18, 102–108. [PubMed: 20934339]

Keuthan CJ, Schaub J, Wei M, Fang W, Quillen S, Kimball E, Johnson TV, Ji H, Zack DJ, Quigley HA, 2023 Sep 6. Regional Gene Expression in the Retina, Optic Nerve Head, and Optic Nerve of Mice with Experimental Glaucoma and Optic Nerve Crush. Int. J. Mol. Sci 24 (18), 13719. 10.3390/ijms241813719. [PubMed: 37762022]

Kielczewski JL, Pease ME, Quigley HA, 2005. The effect of experimental glaucoma and optic nerve transection on amacrine cells in the rat retina. Invest. Ophthalmol. Vis. Sci 46, 3188–3196. [PubMed: 16123418]

Kimball E, Schaub J, Quillen S, Keuthan C, Pease ME, Korneva A, Quigley H, 2021. The role of aquaporin-4 in optic nerve head astrocytes in experimental glaucoma. PLoS One 16, e0244123. [PubMed: 33529207]

Kimball EC, Jefferys JL, Pease ME, Oglesby EN, Nguyen C, Schaub J, Pitha I, Quigley HA, 2018. The effects of age on mitochondria, axonal transport, and axonal degeneration after chronic IOP elevation using a murine ocular explant model. Exp. Eye Res 172, 78–85. [PubMed: 29625080]

Kimball EC, Quillen S, Pease ME, Keuthan C, Nagalingam A, Zack DJ, Johnson TV, Quigley HA, 2022. Aquaporin 4 is not present in normal porcine and human lamina cribrosa. PLoS One 17, e0268541. [PubMed: 35709078]

Kirschner A, Strat AN, Yablonski J, Yoo H, Bague T, Li H, Zhao J, Bollinger KE, Herberg S, Ganapathy PS, 2021. Mechanosensitive channel inhibition attenuates TGFbeta2-induced actin cytoskeletal remodeling and reactivity in mouse optic nerve head astrocytes. Exp. Eye Res 212, 108791. [PubMed: 34656548]

Kirwan RP, Crean JK, Fenerty CH, Clark AF, O'Brien CJ, 2004. Effect of cyclical mechanical stretch and exogenous transforming growth factor-beta1 on matrix metalloproteinase-2 activity in lamina cribrosa cells from the human optic nerve head. J. Glaucoma 13, 327–334. [PubMed: 15226662]

Kirwan RP, Felice L, Clark AF, O'Brien CJ, Leonard MO, 2012. Hypoxia regulated gene transcription in human optic nerve lamina cribrosa cells in culture. Invest. Ophthalmol. Vis. Sci 53, 2243–2255. [PubMed: 22427556]

Kirwan RP, Wordinger RJ, Clark AF, O'Brien CJ, 2009. Differential global and extra-cellular matrix focused gene expression patterns between normal and glaucomatous human lamina cribrosa cells. Mol. Vis 15, 76–88. [PubMed: 19145252]

Kleinschmidt EG, Schlaepfer DD, 2017. Focal adhesion kinase signaling in unexpected places. Curr. Opin. Cell Biol 45, 24–30. [PubMed: 28213315]

Knopp RC, Banks WA, Erickson MA, 2022. Physical associations of microglia and the vascular blood-brain barrier and their importance in development, health, and disease. Curr. Opin. Neurobiol 77, 102648. [PubMed: 36347075]

Konopka A, Zeug A, Skupien A, Kaza B, Mueller F, Chwedorowicz A, Ponimaskin E, Wilczynski GM, Dzwonek J, 2016. Cleavage of hyaluronan and CD44 adhesion molecule regulate astrocyte morphology via Rac1 signalling. PLoS One 11, eOl55053.

Korneva A, Kimball EC, Jefferys JL, Quigley HA, Nguyen TD, 2020. Biomechanics of the optic nerve head and peripapillary sclera in a mouse model of glaucoma. J. R. Soc. Interface 17, 20200708. [PubMed: 33323053]

Korneva A, Kimball EC, Quillen S, Jefferys JL, Nawathe M, Ling YTT, Nguyen TD, Quigley HA, 2022. Mechanical strain in the mouse astrocytic lamina increases after exposure to recombinant trypsin. Acta Biomater.

Kurtenbach S, Kurtenbach S, Zoidl G, 2014. Emerging functions of pannexin 1 in the eye. Front. Cell. Neurosci 8, 263. [PubMed: 25309318]

Lam TT, Kwong JM, Tso MO, 2003. Early glial responses after acute elevated intraocular pressure in rats. Invest. Ophthalmol. Vis. Sci 44, 638–645. [PubMed: 12556393]

Leduc C, Etienne-Manneville S, 2017. Regulation of microtubule-associated motors drives intermediate filament network polarization. J. Cell Biol 216, 1689–1703. [PubMed: 28432079]

Lee SM, Nguyen TH, Na K, Cho IJ, Woo DH, Oh JE, Lee CJ, Yoon ES, 2015. Nanomechanical measurement of astrocyte stiffness correlated with cytoskeletal maturation. J. Biomed. Mater. Res 103, 365–370.

Lee Y, Morrison BM, Li Y, Lengacher S, Farah MH, Hoffman PN, Liu Y, Tsingalia A, Jin L, Zhang PW, Pellerin L, Magistretti PJ, Rothstein JD, 2012. Oligodendroglia metabolically support axons and contribute to neurodegeneration. Nature 487, 443–448. [PubMed: 22801498]

Leiphart RJ, Chen D, Peredo AP, Loneker AE, Janmey PA, 2019. Mechanosensing at cellular interfaces. Langmuir 35, 7509–7519. [PubMed: 30346180]

Leske MC, 2007. Open-angle glaucoma – an epidemiologic overview. Ophthalmic Epidemiol. 14, 166–172. [PubMed: 17896292]

Leske MC, Hyman L, Hussein M, Heijl A, Bengtsson B, 1999. Comparison of glaucomatous progression between untreated patients with normal-tension glaucoma and patients with therapeutically reduced intraocular pressures. The effectiveness of intraocular pressure reduction in the treatment of normal-tension glaucoma. Am J. Ophthalmol 127, 625–626. [PubMed: 10334369]

Leube RE, Moch M, Windoffer R, 2015. Intermediate filaments and the regulation of focal adhesion. Curr. Opin. Cell Biol 32, 13–20. [PubMed: 25460777]

Levkovitch-Verbin H, Quigley HA, Martin KR, Harizman N, Valenta DF, Pease ME, Melamed S, 2005. The transcription factor c-jun is activated in retinal ganglion cells in experimental rat glaucoma. Exp. Eye Res 80, 663–670. [PubMed: 15862173]

Lewis AH, Cui AF, McDonald MF, Grandl J, 2017. Transduction of repetitive mechanical stimuli by Piezo1 and Piezo2 ion channels. Cell Rep. 19, 2572–2585. [PubMed: 28636944]

Liddelow SA, Guttenplan KA, Clarke LE, Bennett FC, Bohlen CJ, Schirmer L, Bennett ML, Münch AE, Chung WS, Peterson TC, Wilton DK, Frouin A, Napier BA, Panicker N, Kumar M, Buckwalter MS, Rowitch DH, Dawson VL, Dawson TM, Stevens B, Barres BA, 2017. Neurotoxic reactive astrocytes are induced by activated microglia. Nature 541, 481–487. [PubMed: 28099414]

Ling YTT, Pease ME, Jefferys JL, Kimball EC, Quigley HA, Nguyen TD, 2020. Pressure-induced changes in astrocyte GFAP, actin, and nuclear morphology in mouse optic nerve. Invest. Ophthalmol. Vis. Sci 61, 14.

Ling YTT, Shi R, Midgett DE, Jefferys JL, Quigley HA, Nguyen TD, 2019. Characterizing the collagen network structure and pressure-induced strains of the human lamina cribrosa. Invest. Ophthalmol. Vis. Sci 60.

Lingor P, Koeberle P, Kugler S, Bahr M, 2005. Down-regulation of apoptosis mediators by RNAi inhibits axotomy-induced retinal ganglion cell death in vivo. Brain 128, 550–558. [PubMed: 15659426]

Liu B, Kilpatrick JI, Lukasz B, Jarvis SP, McDonnell F, Wallace DM, Clark AF, O'Brien CJ, 2018a. Increased substrate stiffness elicits a myofibroblastic phenotype in human lamina cribrosa cells. Invest. Ophthalmol. Vis. Sci 59, 803–814. [PubMed: 29392327]

Liu B, McNally S, Kilpatrick JI, Jarvis SP, O'Brien CJ, 2018b. Aging and ocular tissue stiffness in glaucoma. Surv. Ophthalmol 63, 56–74. [PubMed: 28666629]

Liu F, Lagares D, Choi KM, Stopfer L, Marinkovic A, Vrbanac V, Probst CK, Hiemer SE, Sisson TH, Horowitz JC, Rosas IO, Fredenburgh LE, Feghali-Bostwick C, Varelas X, Tager AM, Tschumperlin DJ, 2015. Mechanosignaling through YAP and TAZ drives fibroblast activation and fibrosis. Am. J. Physiol. Lung Cell Mol. Physiol 308, L344–L357. [PubMed: 25502501]

Lunde LK, Camassa LM, Hoddevik EH, Khan FH, Ottersen OP, Boldt HB, Amiry-Moghaddam M, 2015. Postnatal development of the molecular complex underlying astrocyte polarization. Brain Struct. Funct 220, 2087–2101. [PubMed: 24777283]

Lye-Barthel M, Sun D, Jakobs TC, 2013. Morphology of astrocytes in a glaucomatous optic nerve. Invest. Ophthalmol. Vis. Sci 54, 909–917. [PubMed: 23322566]

Mandal A, Wong HC, Pinter K, Mosqueda N, Beirl A, Lomash RM, Won S, Kindt KS, Drerup CM, 2021. Retrograde mitochondrial transport is essential for organelle distribution and health in zebrafish neurons. J. Neurosci 41, 1371–1392. [PubMed: 33376159]

Maneshi MM, Sachs F, Hua SZ, 2015. A threshold shear force for calcium influx in an astrocyte model of traumatic brain injury. J. Neurotrauma 32, 1020–1029. [PubMed: 25442327]

Maneshi MM, Sachs F, Hua SZ, 2018. Heterogeneous cytoskeletal force distribution delineates the onset Ca(2+) influx under fluid shear stress in astrocytes. Front. Cell. Neurosci 12, 69. [PubMed: 29615869]

Markov P, Zhu H, Boote C, Blain EJ, 2022. Delayed reorganisation of F-actin cytoskeleton and reversible chromatin condensation in scleral fibroblasts under simulated pathological strain. Biochem. Biophys. Rep 32, 101338. [PubMed: 36123992]

Martin KR, Quigley HA, Zack DJ, Levkovitch-Verbin H, Kielczewski J, Valenta D, Baumrind L, Pease ME, Klein RL, Hauswirth WW, 2003. Gene therapy with brain-derived neurotrophic factor as a protection: retinal ganglion cells in a rat glaucoma model. Invest. Ophthalmol. Vis. Sci 44, 4357–4365. [PubMed: 14507880]

Martino F, Perestrelo AR, Vinarsky V, Pagliari S, Forte G, 2018. Cellular mechanotransduction: from tension to function. Front. Physiol 9, 824. [PubMed: 30026699]

Maul EA, Friedman DS, Chang DS, Boland MV, Ramulu PY, Jampel HD, Quigley HA, 2011. Choroidal thickness measured by spectral domain optical coherence tomography: factors affecting thickness in glaucoma patients. Ophthalmology 118, 1571–1579. [PubMed: 21492939]

McBrien NA, Metlapally R, Jobling AI, Gentle A, 2006. Expression of collagen-binding integrin receptors in the mammalian sclera and their regulation during the development of myopia. Invest. Ophthalmol. Vis. Sci 47, 4674–4682. [PubMed: 17065473]

McGlumphy EJ, Mihailovic A, Ramulu PY, Johnson TV, 2021. Home self-tonometry trials compared with clinic tonometry in patients with glaucoma. Ophthalmol. Glaucoma 4, 569–580. [PubMed: 33845191]

McGrady NR, Risner ML, Vest V, Calkins DJ, 2020. TRPV1 tunes optic nerve axon excitability in glaucoma. Front. Physiol 11, 249. [PubMed: 32273850]

Medeiros FA, Zangwill LM, Anderson DR, Liebmann JM, Girkin CA, Harwerth RS, Fredette MJ, Weinreb RN, 2012. Estimating the rate of retinal ganglion cell loss in glaucoma. Am. J. Ophthalmol 154, 814–824 e811. [PubMed: 22840484]

Midgett D, Liu B, Ling YTT, Jefferys JL, Quigley HA, Nguyen TD, 2020a. The effects of glaucoma on the pressure-induced strain response of the human lamina cribrosa. Invest. Ophthalmol. Vis. Sci 61.

Midgett DE, Jefferys JL, Quigley HA, Nguyen TD, 2020b. The inflation response of the human lamina cribrosa and sclera: analysis of deformation and interaction. Acta Biomater. 106, 225–241. [PubMed: 32044458]

Midgett DE, Quigley HA, Nguyen TD, 2019. In vivo characterization of the deformation of the human optic nerve head using optical coherence tomography and digital volume correlation. Acta Biomater. 96.

Miller WJ, Leventhal I, Scarsella D, Haydon PG, Janmey P, Meaney DF, 2009. Mechanically induced reactive gliosis causes ATP-mediated alterations in astrocyte stiffness. J. Neurotrauma 26, 789–797. [PubMed: 19331521]

Minckler DS, Bunt AH, Klock IB, 1978. Radioautographic and cytochemical ultrastructural studies of axoplasmic transport in the monkey optic nerve head. Invest. Ophthalmol. Vis. Sci 17, 33–50. [PubMed: 74368]

Minckler DS, McLean IW, Tso MO, 1976. Distribution of axonal and glial elements in the rhesus optic nerve head studied by electron microscopy. Am. J. Ophthalmol 82, 179–187. [PubMed: 821348]

Mishima S, Maurice DM, 1961. The effect of normal evaporation on the eye. Exp. Eye Res 1, 46–52. [PubMed: 14474547]

Mitra SK, Hanson DA, Schlaepfer DD, 2005. Focal adhesion kinase: in command and control of cell motility. Nat. Rev. Mol. Cell Biol 6, 56–68. [PubMed: 15688067]

Moeton M, Stassen OM, Sluijs JA, van der Meer VW, Kluivers LJ, van Hoorn H, Schmidt T, Reits EA, van Strien ME, Hoi EM, 2016. GFAP isoforms control intermediate filament network dynamics, cell morphology, and focal adhesions. Cell. Mol. Life Sci 73, 4101–4120. [PubMed: 27141937]

Moreels M, Vandenabeele F, Dumont D, Robben J, Lambrichts I, 2008. Alpha-smooth muscle actin (alpha-SMA) and nestin expression in reactive astrocytes in multiple sclerosis lesions: potential regulatory role of transforming growth factor-beta 1 (TGF-beta1). Neuropathol. Appl. Neurobiol 34, 532–546. [PubMed: 18005096]

Morgan JE, 2002. Retinal ganglion cell shrinkage in glaucoma. J. Glaucoma 11, 365–370. [PubMed: 12169976]

Morgan WH, Yu DY, Alder VA, Cringle SJ, Cooper RL, House PH, Constable IJ, 1998. The correlation between cerebrospinal fluid pressure and retrolaminar tissue pressure. Invest. Ophthalmol. Vis. Sci 39, 1419–1428. [PubMed: 9660490]

Morozumi W, Inagaki S, Iwata Y, Nakamura S, Hara H, Shimazawa M, 2020. Piezo channel plays a part in retinal ganglion cell damage. Exp. Eye Res 191, 107900. [PubMed: 31874142]

Morrison JC, 2006. Integrins in the optic nerve head: potential roles in glaucomatous optic neuropathy (an American Ophthalmological Society thesis). Trans. Am. Ophthalmol. Soc 104, 453–477. [PubMed: 17471356]

Morrison JC, Dorman-Pease ME, Dunkelberger GR, Quigley HA, 1990. Optic nerve head extracellular matrix in primary optic atrophy and experimental glaucoma. Arch. Ophthalmol 108, 1020–1024. [PubMed: 2369339]

Morrison JC, Johnson EC, Cepurna W, Jia L, 2005. Understanding mechanisms of pressure-induced optic nerve damage. Prog. Retin. Eye Res 24, 217–240. [PubMed: 15610974]

Mulvihill JJE, Raykin J, Snider EJ, Schildmeyer LA, Zaman I, Platt MO, Kelly DJ, Ethier CR, 2018. Development of a platform for studying 3D astrocyte mechanobiology: compression of astrocytes in collagen gels. Ann. Biomed. Eng 46, 365–374. [PubMed: 29181720]

Murata K, Hirata A, Ohta K, Enaida H, Nakamura KI, 2019. Morphometric analysis in mouse scleral fibroblasts using focused ion beam/scanning electron microscopy. Sci. Rep 9, 6329. [PubMed: 31004111]

Murphy R, Irnaten M, Hopkins A, O'Callaghan J, Stamer WD, Clark AF, Wallace D, O'Brien CJ, 2022. Matrix mechanotransduction via yes-associated protein in human lamina cribrosa cells in glaucoma. Invest. Ophthalmol. Vis. Sci 63, 16.

Myers KM, Cone FE, Quigley HA, Gelman S, Pease ME, Nguyen TD, 2010. The in vitro inflation response of mouse sclera. Exp. Eye Res 91, 866–875. [PubMed: 20868685]

Nagy JI, Rash JE, 2000. Connexins and gap junctions of astrocytes and oligodendrocytes in the CNS. Brain Res. Brain Res. Rev 32, 29–44. [PubMed: 10751655]

Neidlinger-Wilke C, Grood ES, Wang J-C, Brand RA, Claes L, 2001. Cell alignment is induced by cyclic changes in cell length: studies of cells grown in cyclically stretched substrates. J. Orthop. Res 19, 286–293. [PubMed: 11347703]

Nguyen C, Cone FE, Nguyen TD, Coudrillier B, Pease ME, Steinhart MR, Oglesby EN, Jefferys JL, Quigley HA, 2013a. Studies of scleral biomechanical behavior related to susceptibility for retinal ganglion cell loss in experimental mouse glaucoma. Invest. Ophthalmol. Vis. Sci 54, 1767–1780. [PubMed: 23404116]

Nguyen C, Cone FE, Nguyen TD, Coudrillier B, Pease ME, Steinhart MR, Oglesby EN, Jefferys JL, Quigley HA, 2013b. Studies of scleral biomechanical behavior related to susceptibility for retinal ganglion cell loss in experimental mouse glaucoma. Invest. Ophthalmol. Vis. Sci 54.

Niland S, Westerhausen C, Schneider SW, Eckes B, Schneider MF, Eble JA, 2011. Biofunctionalization of a generic collagenous triple helix with the alpha2beta1 integrin binding site allows molecular force measurements. Int. J. Biochem. Cell Biol 43, 721–731. [PubMed: 21262375]

Nishimura Y, Kasahara K, Inagaki M, 2019. Intermediate filaments and IF-associated proteins: from cell architecture to cell proliferation. Proc. Jpn. Acad. Ser. B Phys. Biol. Sci 95, 479–493.

Norman RE, Flanagan JG, Sigal IA, Rausch SMK, Tertinegg I, Ethier CR, 2011. Finite element modeling of the human sclera: influence on optic nerve head biomechanics and connections with glaucoma. Exp. Eye Res 93.

Nouri-Mahdavi K, Hoffman D, Coleman AL, Liu G, Li G, Gaasterland D, Caprioli J, Advanced Glaucoma Intervention S., 2004. Predictive factors for glaucomatous visual field progression in the Advanced Glaucoma Intervention Study. Ophthalmology 111, 1627–1635. [PubMed: 15350314]

Oglesby EN, Tezel G, Cone-Kimball E, Steinhart MR, Jefferys J, Pease ME, Quigley HA, 2016. Scleral fibroblast response to experimental glaucoma in mice. Mol. Vis 22, 82–99. [PubMed: 26900327]

Ostrow LW, Suchyna TM, Sachs F, 2011. Stretch induced endothelin-1 secretion by adult rat astrocytes involves calcium influx via stretch-activated ion channels (SACs). Biochem. Biophys. Res. Commun 410, 81–86. [PubMed: 21640709]

Ou Y, Jo RE, Ullian EM, Wong RO, Della Santina L, 2016. Selective vulnerability of specific retinal ganglion cell types and synapses after transient ocular hypertension. J. Neurosci 36, 9240–9252. [PubMed: 27581463]

Pardo-Pastor C, Rubio-Moscardo F, Vogel-Gonzalez M, Serra SA, Afthinos A, Mrkonjic S, Destaing O, Abenza JF, Fernandez-Fernandez JM, Trepat X, Albiges-Rizo C, Konstantopoulos K, Valverde MA, 2018. Piezo2 channel regulates RhoA and actin cytoskeleton to promote cell mechanobiological responses. Proc. Natl. Acad. Sci. U.S.A 115, 1925–1930. [PubMed: 29432180]

Parton RG, del Pozo MA, 2013. Caveolae as plasma membrane sensors, protectors and organizers. Nat. Rev. Mol. Cell Biol 14, 98–112. [PubMed: 23340574]

Pasapera AM, Schneider IC, Rericha E, Schlaepfer DD, Waterman CM, 2010. Myosin II activity regulates vinculin recruitment to focal adhesions through FAK-mediated paxillin phosphorylation. J. Cell Biol 188, 877–890. [PubMed: 20308429]

Pazos M, Yang H, Gardiner SK, Cepurna WO, Johnson EC, Morrison JC, Burgoyne CF, 2015. Rat optic nerve head anatomy within 3D histomorphometric reconstructions of normal control eyes. Exp. Eye Res 139, 1–12. [PubMed: 26021973]

Pazos M, Yang H, Gardiner SK, Cepurna WO, Johnson EC, Morrison JC, Burgoyne CF, 2016. Expansions of the neurovascular scleral canal and contained optic nerve occur early in the hypertonic saline rat experimental glaucoma model. Exp. Eye Res 145, 173–186. [PubMed: 26500195]

Pease ME, McKinnon SJ, Quigley HA, Kerrigan-Baumrind LA, Zack DJ, 2000. Obstructed axonal transport of BDNF and its receptor TrkB in experimental glaucoma. Invest. Ophthalmol. Vis. Sci 41, 764–774. [PubMed: 10711692]

Pekny M, 2001. Astrocytic intermediate filaments: lessons from GFAP and vimentin knock-out mice. Prog. Brain Res 132, 23–30. [PubMed: 11544992]

Pellerin L, Pellegri G, Bittar PG, Charnay Y, Bouras C, Martin JL, Stella N, Magistretti PJ, 1998. Evidence supporting the existence of an activity-dependent astrocyte-neuron lactate shuttle. Dev. Neurosci 20, 291–299. [PubMed: 9778565]

Perry VH, Henderson Z, Linden R, 1983. Postnatal changes in retinal ganglion cell and optic axon populations in the pigmented rat. J. Comp. Neurol 219, 356–368. [PubMed: 6619343]

Pierre K, Pellerin L, Debernardi R, Riederer BM, Magistretti PJ, 2000. Cell-specific localization of monocarboxylate transporters, MCT1 and MCT2, in the adult mouse brain revealed by double immunohistochemical labeling and confocal microscopy. Neuroscience 100, 617–627. [PubMed: 11098125]

Piersma B, de Rond S, Werker PM, Boo S, Hinz B, van Beuge MM, Bank RA, 2015. YAP1 is a driver of myofibroblast differentiation in normal and diseased fibroblasts. Am. J. Pathol 185, 3326–3337. [PubMed: 26458763]

Pijanka JK, Coudrillier B, Ziegler K, Sorensen T, Meek KM, Nguyen TD, Quigley HA, Boote C, 2012. Quantitative mapping of collagen fiber orientation in non-glaucoma and glaucoma posterior human sclerae. Invest. Ophthalmol. Vis. Sci 53.

Pijanka JK, Kimball EC, Pease ME, Abass A, Sorensen T, Nguyen TD, Quigley HA, Boote C, 2014. Changes in scleral collagen organization in murine chronic experimental glaucoma. Invest. Ophthalmol. Vis. Sci 55.

Pijanka JK, Spang MT, Sorensen T, Liu J, Nguyen TD, Quigley HA, Boote C, 2015. Depth-dependent changes in collagen organization in the human peripapillary sclera. PLoS One 10, e0118648. [PubMed: 25714753]

Pitha I, Oglesby E, Chow A, Kimball E, Pease ME, Schaub J, Quigley H, 2018. Rho-kinase inhibition reduces myofibroblast differentiation and proliferation of scleral fibroblasts induced by transforming growth factor beta and experimental glaucoma. Transl. Vis. Sci. Technol 7, 6.

Prager-Khoutorsky M, Lichtenstein A, Krishnan R, Rajendran K, Mayo A, Kam Z, Geiger B, Bershadsky AD, 2011. Fibroblast polarization is a matrix-rigidity-dependent process controlled by focal adhesion mechanosensing. Nat. Cell Biol 13, 1457–1465. [PubMed: 22081092]

Qiu C, Chen M, Yao J, Sun X, Xu J, Zhang R, Wang X, Li G, Qian S, 2018. Mechanical strain induces distinct human scleral fibroblast lineages: differential roles in cell proliferation, apoptosis, migration, and differentiation. Invest. Ophthalmol. Vis. Sci 59, 2401–2410. [PubMed: 29847646]

Qiu C, Wang C, Sun X, Xu J, Wu J, Zhang R, Li G, Xue K, Zhang X, Qian S, 2022. CXC-receptor 2 promotes extracellular matrix production and attenuates migration in peripapillary human scleral fibroblasts under mechanical strain. J. Cell Mol. Med 26, 5858–5871. [PubMed: 36349481]

Qu J, Chen H, Zhu L, Ambalavanan N, Girkin CA, Murphy-Ullrich JE, Downs JC, Zhou Y, 2015. High-magnitude and/or high-frequency mechanical strain promotes peripapillary scleral myofibroblast differentiation. Invest. Ophthalmol. Vis. Sci 56, 7821–7830. [PubMed: 26658503]

Quigley H, Anderson DR, 1976. The dynamics and location of axonal transport blockade by acute intraocular pressure elevation in primate optic nerve. Invest. Ophthalmol 15, 606–616. [PubMed: 60300]

Quigley HA, 1977a. Gap junctions between optic nerve head astrocytes. Invest. Ophthalmol. Vis. Sci 16, 582–585. [PubMed: 405347]

Quigley HA, 1977b. The pathogenesis of reversible cupping in congenital glaucoma. Am. J. Ophthalmol 84, 358–370. [PubMed: 900230]

Quigley HA, 2015. The Contribution of the Sclera and Lamina Cribrosa to the Pathogenesis of Glaucoma: Diagnostic and Treatment Implications.

Quigley HA, 2016. Understanding glaucomatous optic neuropathy: the synergy between clinical observation and investigation. Annu. Rev. Vis. Sci 2, 235–254. [PubMed: 28532352]

Quigley HA, Addicks EM, 1980. Chronic experimental glaucoma in primates. II. Effect of extended intraocular pressure elevation on optic nerve head and axonal transport. Invest. Ophthalmol. Vis. Sci 19, 137–152. [PubMed: 6153173]

Quigley HA, Addicks EM, 1981. Regional differences in the structure of the lamina cribrosa and their relation to glaucomatous optic nerve damage. Arch. Ophthalmol 99, 137–143. [PubMed: 7458737]

Quigley HA, Addicks EM, Green WR, 1982. Optic nerve damage in human glaucoma. III. Quantitative correlation of nerve fiber loss and visual field defect in glaucoma, ischemic neuropathy, papilledema, and toxic neuropathy. Arch. Ophthalmol 100, 135–146. [PubMed: 7055464]

Quigley HA, Addicks EM, Green WR, Maumenee AE, 1981. Optic nerve damage in human glaucoma. II. The site of injury and susceptibility to damage. Arch. Ophthalmol 99, 635–649. [PubMed: 6164357]

Quigley HA, Anderson DR, 1977. The histologic basis of optic disk pallor in experimental optic atrophy. Am. J. Ophthalmol 83, 709–717. [PubMed: 405870]

Quigley HA, Brown A, Dorman-Pease ME, 1991a. Alterations in elastin of the optic nerve head in human and experimental glaucoma. Br. J. Ophthalmol 75.

Quigley HA, Dorman-Pease ME, Brown AE, 1991b. Quantitative study of collagen and elastin of the optic nerve head and sclera in human and experimental monkey glaucoma. Curr. Eye Res 10.

Quigley HA, Dunkelberger GR, Green WR, 1988. Chronic human glaucoma causing selectively greater loss of large optic nerve fibers. Ophthalmology 95, 357–363. [PubMed: 3174003]

Quigley HA, Dunkelberger GR, Green WR, 1989. Retinal ganglion cell atrophy correlated with automated perimetry in human eyes with glaucoma. Am. J. Ophthalmol 107, 453–464. [PubMed: 2712129]

Quigley HA, Flower RW, Addicks EM, McLeod DS, 1980. The mechanism of optic nerve damage in experimental acute intraocular pressure elevation. Invest. Ophthalmol. Vis. Sci 19, 505–517. [PubMed: 6154668]

Quigley HA, Green WR, 1979. The histology of human glaucoma cupping and optic nerve damage: clinicopathologic correlation in 21 eyes. Ophthalmology 86, 1803–1830. [PubMed: 553256]

Quigley HA, Hohman RM, Addicks EM, Green WR, 1984. Blood vessels of the glaucomatous optic disc in experimental primate and human eyes. Invest. Ophthalmol. Vis. Sci 25, 918–931. [PubMed: 6746235]

Quigley HA, Hohman RM, Addicks EM, Massof RW, Richard Green W, 1983. Morphologic changes in the lamina cribrosa correlated with neural loss in open-angle glaucoma. Am. J. Ophthalmol 95.

Quigley HA, Hohman RM, Sanchez R, Addicks EM, 1985. Optic nerve head blood flow in chronic experimental glaucoma. Arch. Ophthalmol 103, 956–962. [PubMed: 4015488]

Quigley HA, Nickells RW, Kerrigan LA, Pease ME, Thibault DJ, Zack DJ, 1995. Retinal ganglion cell death in experimental glaucoma and after axotomy occurs by apoptosis. Invest. Ophthalmol. Vis. Sci 36, 774–786. [PubMed: 7706025]

Quigley HA, Sanchez RM, Dunkelberger GR, L'Hernault NL, Baginski TA, 1987. Chronic glaucoma selectively damages large optic nerve fibers. Invest. Ophthalmol. Vis. Sci 28, 913–920. [PubMed: 3583630]

Quill B, Docherty NG, Clark AF, O'Brien CJ, 2011. The effect of graded cyclic stretching on extracellular matrix-related gene expression profiles in cultured primary human lamina cribrosa cells. Invest. Ophthalmol. Vis. Sci 52, 1908–1915. [PubMed: 21169532]

Quill B, Irnaten M, Docherty NG, McElnea EM, Wallace DM, Clark AF, O'Brien CJ, 2015. Calcium channel blockade reduces mechanical strain-induced extracellular matrix gene response in lamina cribrosa cells. Br. J. Ophthalmol 99, 1009–1014. [PubMed: 25795916]

Quillen S, Schaub J, Quigley H, Pease M, Korneva A, Kimball E, 2020. Astrocyte responses to experimental glaucoma in mouse optic nerve head. PLoS One 15, e0238104. [PubMed: 32822415]

Radius RL, Maumenee AE, Green WR, 1978. Pit-like changes of the optic nerve head in open-angle glaucoma. Br. J. Ophthalmol 62, 389–393. [PubMed: 666988]

Raff MC, Barres BA, Burne JF, Coles HS, Ishizaki Y, Jacobson MD, 1993. Programmed cell death and the control of cell survival: lessons from the nervous system. Science 262, 695–700. [PubMed: 8235590]

Rahikainen R, Ohman T, Turkki P, Varjosalo M, Hytonen VP, 2019. Talin-mediated force transmission and talin rod domain unfolding independently regulate adhesion signaling. J. Cell Sci 132.

Raviola G, Sagaties MJ, Miller C, 1987. Intercellular junctions between fibroblasts in connective tissues of the eye of macaque monkeys. A thin section and freeze fracture analysis. Invest. Ophthalmol. Vis. Sci 28, 834–841. [PubMed: 3570693]

Realini T, Weinreb RN, Wisniewski S, 2011. Short-term repeatability of diurnal intraocular pressure patterns in glaucomatous individuals. Ophthalmology 118, 47–51. [PubMed: 20709404]

Ren R, Wang N, Li B, Li L, Gao F, Xu X, Jonas JB, 2009. Lamina cribrosa and peripapillary sclera histomorphometry in normal and advanced glaucomatous Chinese eyes with various axial length. Investig. Ophthalmol. Visual Sci 50.

rho Gould RA, Yalcin HC, MacKay JL, Sauls K, Norris R, Kumar S, Butcher JT, 2016. Cyclic mechanical loading is essential for rac1-mediated elongation and remodeling of the embryonic mitral valve. Curr. Biol 26, 27–37. [PubMed: 26725196]

Roberts MD, Grau V, Grimm J, Reynaud J, Bellezza AJ, Burgoyne CF, Downs JC, 2009. Remodeling of the connective tissue microarchitecture of the lamina cribrosa in early experimental glaucoma. Invest. Ophthalmol. Vis. Sci 50.

Rosas-Hernandez R, Bastian Y, Juarez Tello A, Ramirez-Saito A, Escobar Garcia DM, Pozos-Guillen A, Mendez JA, 2019. AMPA receptors modulate the reorganization of F-actin in Bergmann glia cells through the activation of RhoA. J. Neurochem 149, 242–254. [PubMed: 30589940]

Rosengren B, 1950. Studies in depth of the anterior chamber of the eye in primary glaucoma. AMA Arch. Ophthalmol 44, 523–538. [PubMed: 14770649]

Salinas-Navarro M, Alarcon-Martinez L, Valiente-Soriano FJ, Jimenez-Lopez M, Mayor-Torroglosa S, Aviles-Trigueros M, Villegas-Perez MP, Vidal-Sanz M, 2010. Ocular hypertension impairs optic nerve axonal transport leading to progressive retinal ganglion cell degeneration. Exp. Eye Res 90, 168–183. [PubMed: 19835874]

Sappington RM, Sidorova T, Long DJ, Calkins DJ, 2009. TRPV1: contribution to retinal ganglion cell apoptosis and increased intracellular Ca2+ with exposure to hydrostatic pressure. Invest. Ophthalmol. Vis. Sci 50, 717–728. [PubMed: 18952924]

Seetharaman S, Etienne-Manneville S, 2018. Integrin diversity brings specificity in mechanotransduction. Biol. Cell 110, 49–64. [PubMed: 29388220]

Segel M, Neumann B, Hill MFE, Weber IP, Viscomi C, Zhao C, Young A, Agley CC, Thompson AJ, Gonzalez GA, Sharma A, Holmqvist S, Rowitch DH, Franze K, Franklin RJM, Chalut KJ, 2019. Niche stiffness underlies the ageing of central nervous system progenitor cells. Nature 573, 130–134. [PubMed: 31413369]

Shelton L, Rada JA, 2009. Inhibition of human scleral fibroblast cell attachment to collagen type I by TGFBIp. Invest. Ophthalmol. Vis. Sci 50, 3542–3552. [PubMed: 19387070]

Shuba LM, Doan AP, Maley MK, Zimmerman MB, Dinn RB, Greenlee EC, Alward WL, Kwon YH, 2007. Diurnal fluctuation and concordance of intraocular pressure in glaucoma suspects and normal tension glaucoma patients. J. Glaucoma 16, 307–312. [PubMed: 17438425]

Sigal IA, Ethier CR, 2009. Biomechanics of the optic nerve head. Exp. Eye Res 88, 799–807. [PubMed: 19217902]

Silver DM, Quigley HA, 2004. Aqueous flow through the iris-lens channel: estimates of differential pressure between the anterior and posterior chambers. J. Glaucoma 13, 100–107. [PubMed: 15097254]

Sit AJ, Nau CB, McLaren JW, Johnson DH, Hodge D, 2008. Circadian variation of aqueous dynamics in young healthy adults. Invest. Ophthalmol. Vis. Sci 49, 1473–1479. [PubMed: 18385065]

Sommer A, 2011. Ocular hypertension and normal-tension glaucoma: time for banishment and burial. Arch. Ophthalmol 129, 785–787. [PubMed: 21670346]

Sommer A, Tielsch JM, Katz J, Quigley HA, Gottsch JD, Javitt J, Singh K, 1991. Relationship between intraocular pressure and primary open angle glaucoma among white and black Americans. The Baltimore Eye Survey. Arch. Ophthalmol 109, 1090–1095. [PubMed: 1867550]

Sun H, Wang Y, Pang IH, Shen J, Tang X, Li Y, Liu C, Li B, 2011. Protective effect of a JNK inhibitor against retinal ganglion cell loss induced by acute moderate ocular hypertension. Mol. Vis 17, 864–875. [PubMed: 21527996]

Szeto J, Chow A, McCrea L, Mozzer A, Nguyen TD, Quigley HA, Pitha I, 2021. Regional differences and physiologic behaviors in peripapillary scleral fibroblasts. Invest. Ophthalmol. Vis. Sci 62, 27.

Szurman P, Gillmann K, Seuthe AM, Dick HB, Hoffmann EM, Mermoud A, Mackert MJ, Weinreb RN, Rao HL, Mansouri K, Group E-SS, 2023. EYEMATE-SC trial: twelve-month safety, performance, and accuracy of a suprachoroidal sensor for telemetric measurement of intraocular pressure. Ophthalmology 130, 304–312. [PubMed: 36202141]

Tamiello C, Bouten CV, Baaijens FP, 2015. Competition between cap and basal actin fiber orientation in cells subjected to contact guidance and cyclic strain. Sci. Rep 5, 8752. [PubMed: 25736393]

Tapia-Rojo R, Alonso-Caballero A, Fernandez JM, 2020. Talin folding as the tuning fork of cellular mechanotransduction. Proc. Natl. Acad. Sci. U.S.A 117, 21346–21353. [PubMed: 32817549]

Tehrani S, Davis L, Cepurna WO, Choe TE, Lozano DC, Monfared A, Cooper L, Cheng J, Johnson EC, Morrison JC, 2016. Astrocyte structural and molecular response to elevated intraocular

pressure occurs rapidly and precedes axonal tubulin rearrangement within the optic nerve head in a rat model. PLoS One 11, e0167364. [PubMed: 27893827]

Tehrani S, Davis L, Cepurna WO, Delf RK, Lozano DC, Choe TE, Johnson EC, Morrison JC, 2019. Optic nerve head astrocytes display axon-dependent and -independent reactivity in response to acutely elevated intraocular pressure. Invest. Ophthalmol. Vis. Sci 60, 312–321. [PubMed: 30665231]

Tehrani S, Johnson EC, Cepurna WO, Morrison JC, 2014. Astrocyte processes label for filamentous actin and reorient early within the optic nerve head in a rat glaucoma model. Invest. Ophthalmol. Vis. Sci 55, 6945–6952. [PubMed: 25257054]

Tekkok SB, Brown AM, Westenbroek R, Pellerin L, Ransom BR, 2005. Transfer of glycogen-derived lactate from astrocytes to axons via specific monocarboxylate transporters supports mouse optic nerve activity. J. Neurosci. Res 81, 644–652. [PubMed: 16015619]

Tezel G, Chauhan BC, LeBlanc RP, Wax MB, 2003. Immunohistochemical assessment of the glial mitogen-activated protein kinase activation in glaucoma. Invest. Ophthalmol. Vis. Sci 44, 3025–3033. [PubMed: 12824248]

Thomas WE, Vogel V, Sokurenko E, 2008. Biophysics of catch bonds. Annu. Rev. Biophys 37, 399–416. [PubMed: 18573088]

Tielsch JM, Katz J, Sommer A, Quigley HA, Javitt JC, 1995. Hypertension, perfusion pressure, and primary open-angle glaucoma. A population-based assessment. Arch. Ophthalmol 113, 216–221. [PubMed: 7864755]

Tovar-Vidales T, Wordinger RJ, Clark AF, 2016. Identification and localization of lamina cribrosa cells in the human optic nerve head. Exp. Eye Res 147, 94–97. [PubMed: 27167365]

Tso MO, Shih CY, McLean IW, 1975. Is there a blood-brain barrier at the optic nerve head? Arch. Ophthalmol 93, 815–825. [PubMed: 828849]

Turner DC, Girkin CA, Downs JC, 2019a. The magnitude of intraocular pressure elevation associated with eye rubbing. Ophthalmology 126, 171–172. [PubMed: 30153437]

Turner DC, Miranda M, Morris JS, Girkin CA, Downs JC, 2019b. Acute stress increases intraocular pressure in nonhuman primates. Ophthalmol. Glaucoma 2, 210–214. [PubMed: 31799505]

Uemura A, Nguyen TN, Steele AN, Yamada S, 2011. The LIM domain of zyxin is sufficient for force-induced accumulation of zyxin during cell migration. Biophys. J 101, 1069–1075. [PubMed: 21889443]

van Putten S, Shafieyan Y, Hinz B, 2016. Mechanical control of cardiac myofibroblasts. J. Mol. Cell. Cardiol 93, 133–142. [PubMed: 26620422]

Vedrenne N, Sarrazy V, Richard L, Bordeau N, Battu S, Billet F, Desmouliere A, 2017. Isolation of astrocytes displaying myofibroblast properties and present in multiple sclerosis lesions. Neurochem. Res 42, 2427–2434. [PubMed: 28434162]

Wang B, Nevins JE, Nadler Z, Wollstein G, Ishikawa H, Bilonick RA, Kagemann L, Sigal IA, Grulkowski I, Liu JJ, Kraus M, Lu CD, Hornegger J, Fujimoto JG, Schuman JS, 2013. In vivo lamina cribrosa micro-architecture in healthy and glaucomatous eyes as assessed by optical coherence tomography. Invest. Ophthalmol. Vis. Sci 54.

Wang JH, Grood ES, 2000. The strain magnitude and contact guidance determine orientation response of fibroblasts to cyclic substrate strains. Connect. Tissue Res 41, 29–36. [PubMed: 10826706]

Wang R, Seifert P, Jakobs TC, 2017. Astrocytes in the optic nerve head of glaucomatous mice display a characteristic reactive phenotype. Invest. Ophthalmol. Vis. Sci 58, 924–932. [PubMed: 28170536]

Wang X, Tay SS, Ng YK, 2000. An immunohistochemical study of neuronal and glial cell reactions in retinae of rats with experimental glaucoma. Exp. Brain Res 132, 476–484. [PubMed: 10912828]

Weinreb RN, Aung T, Medeiros FA, 2014. The pathophysiology and treatment of glaucoma: a review. JAMA 311, 1901–1911. [PubMed: 24825645]

Welsbie DS, Yang Z, Ge Y, Mitchell KL, Zhou X, Martin SE, Berlinicke CA, Hackler L Jr., Fuller J, Fu J, Cao LH, Han B, Auld D, Xue T, Hirai S, Germain L, Simard-Bisson C, Blouin R, Nguyen JV, Davis CH, Enke RA, Boye SL, Merbs SL, Marsh-Armstrong N, Hauswirth WW, DiAntonio A, Nickells RW, Inglese J, Hanes J, Yau KW, Quigley HA, Zack DJ, 2013. Functional genomic

screening identifies dual leucine zipper kinase as a key mediator of retinal ganglion cell death. Proc. Natl. Acad. Sci. U.S.A 110, 4045–4050. [PubMed: 23431148]

Wilensky JT, Zeimer RC, Gieser DK, Kaplan BH, 1994. The effects of glaucoma filtering surgery on the variability of diurnal intraocular pressure. Trans. Am. Ophthalmol. Soc 92, 377–381 discussion 381-373. [PubMed: 7886873]

Wong VW, Rustad KC, Akaishi S, Sorkin M, Glotzbach JP, Januszyk M, Nelson ER, Levi K, Paterno J, Vial IN, Kuang AA, Longaker MT, Gurtner GC, 2011. Focal adhesion kinase links mechanical force to skin fibrosis via inflammatory signaling. Nat. Med 18, 148–152. [PubMed: 22157678]

Xie Y, Ouyang X, Wang G, 2020. Mechanical strain affects collagen metabolism-related gene expression in scleral fibroblasts. Biomed. Pharmacother 126, 110095. [PubMed: 32217440]

Yamamoto K, Maruyama K, Himori N, Omodaka K, Yokoyama Y, Shiga Y, Morin R, Nakazawa T, 2014. The novel Rho kinase (ROCK) inhibitor K-115: a new candidate drug for neuroprotective treatment in glaucoma. Invest. Ophthalmol. Vis. Sci 55, 7126–7136. [PubMed: 25277230]

Yamaoka A, Matsuo T, Shiraga F, Ohtsuki H, 2001. TIMP-1 production by human scleral fibroblast decreases in response to cyclic mechanical stretching. Ophthalmic Res. 33, 98–101. [PubMed: 11244355]

Yang D, Liu JHK, Wang N, Weinreb RN, 2020. Correlation between office-hour and peak nocturnal intraocular pressure in patients treated with prostaglandin analogs. Am. J. Ophthalmol 215, 112–117. [PubMed: 32087142]

Yang H, Downs JC, Girkin C, Sakata L, Bellezza A, Thompson H, Burgoyne CF, 2007a. 3-D histomorphometry of the normal and early glaucomatous monkey optic nerve head: lamina cribrosa and peripapillary scleral position and thickness. Invest. Ophthalmol. Vis. Sci 48.

Yang H, Reynaud J, Lockwood H, Williams G, Hardin C, Reyes L, Stowell C, Gardiner SK, Burgoyne CF, 2017. The connective tissue phenotype of glaucomatous cupping in the monkey eye. Clin. Res. Impl

Yang H, Williams G, Crawford Downs J, Sigal IA, Roberts MD, Thompson H, Burgoyne CF, 2011. Posterior (outward) migration of the lamina cribrosa and early cupping in monkey experimental glaucoma. Invest. Ophthalmol. Vis. Sci 52.

Yang Z, Quigley HA, Pease ME, Yang Y, Qian J, Valenta D, Zack DJ, 2007b. Changes in gene expression in experimental glaucoma and optic nerve transection: the equilibrium between protective and detrimental mechanisms. Invest. Ophthalmol. Vis. Sci 48, 5539–5548. [PubMed: 18055803]

Yang Z, Wang KK, 2015. Glial fibrillary acidic protein: from intermediate filament assembly and gliosis to neurobiomarker. Trends Neurosci. 38, 364–374. [PubMed: 25975510]

Yuan Y, Li M, To CH, Lam TC, Wang P, Yu Y, Chen Q, Hu X, Ke B, 2018. The role of the RhoA/ROCK signaling pathway in mechanical strain-induced scleral myofibroblast differentiation. Invest. Ophthalmol. Vis. Sci 59, 3619–3629. [PubMed: 30029249]

Yuan Z, Czerpak CA, Kashaf MS, Quigley HA, Nguyen TD, 2023. Biomechanical Strain Responses in the Optic Nerve Head Region in Glaucoma Patients after Intraocular Pressure Lowering. medRxiv.

Zhang N, He X, Xing Y, Yang N, 2022. Differential susceptibility of retinal ganglion cell subtypes against neurodegenerative diseases. Graefes Arch. Clin. Exp. Ophthalmol 260, 1807–1821. [PubMed: 35038014]

Zhou J, Aponte-Santamaria C, Sturm S, Bullerjahn JT, Bronowska A, Grater F, 2015. Mechanism of focal adhesion kinase mechanosensing. PLoS Comput. Biol 11, e1004593. [PubMed: 26544178]

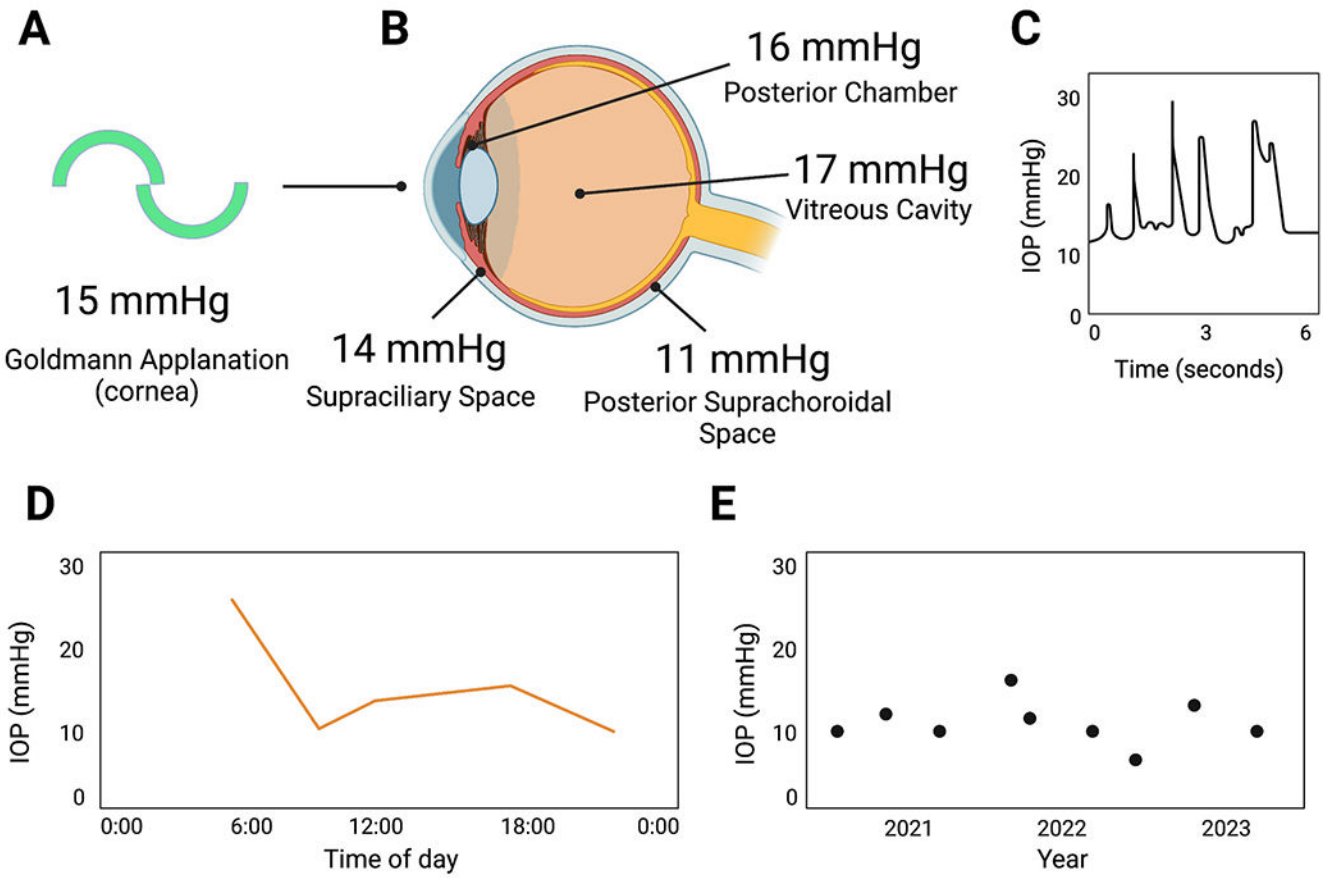

Fig. 1. Sources of IOP variation.

Clinical decision making in glaucoma most often uses isolated measurements (A) or measurements separated by months (E) and all IOP measurements are taken at the surface of the cornea. (B) IOP levels within the eye vary regionally due to pressure gradients that drive fluid flow. IOP level is dynamic with variations that can be seen within a span of several seconds (C), over the course of a day (D), and over months during regular clinical visits (E).

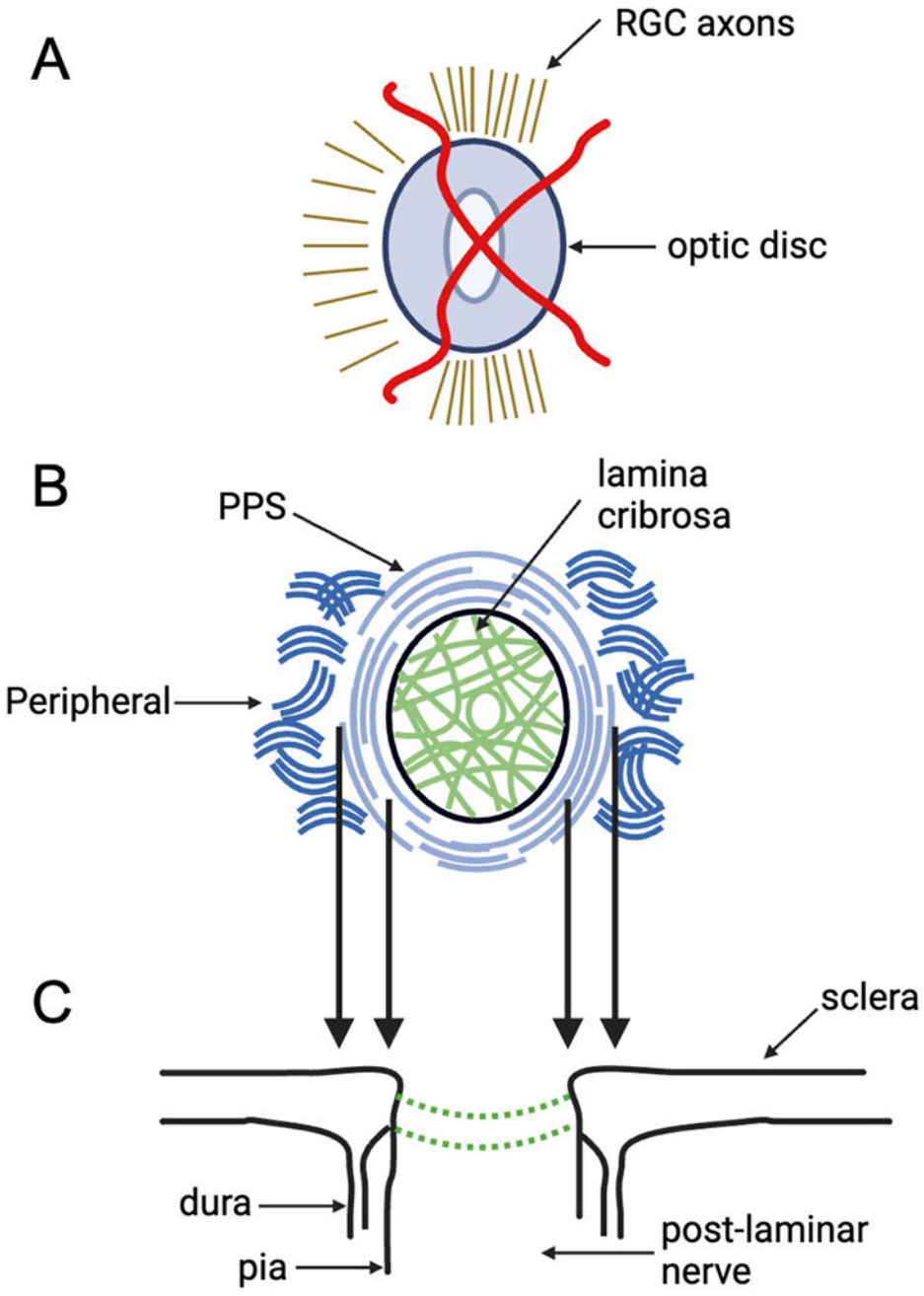

Fig. 2. Connective tissue components of the optic nerve head.

Illustration of the optic disc (A) and the connective tissue components of the optic nerve head (B) showing the circumferentially arrange collagen lamellae of the peripapillary sclera (PPS), the basket weaved pattern of the peripheral sclera, and lamina cribrosa. These structures form the ONH through which RGC axons exit the eye (C).

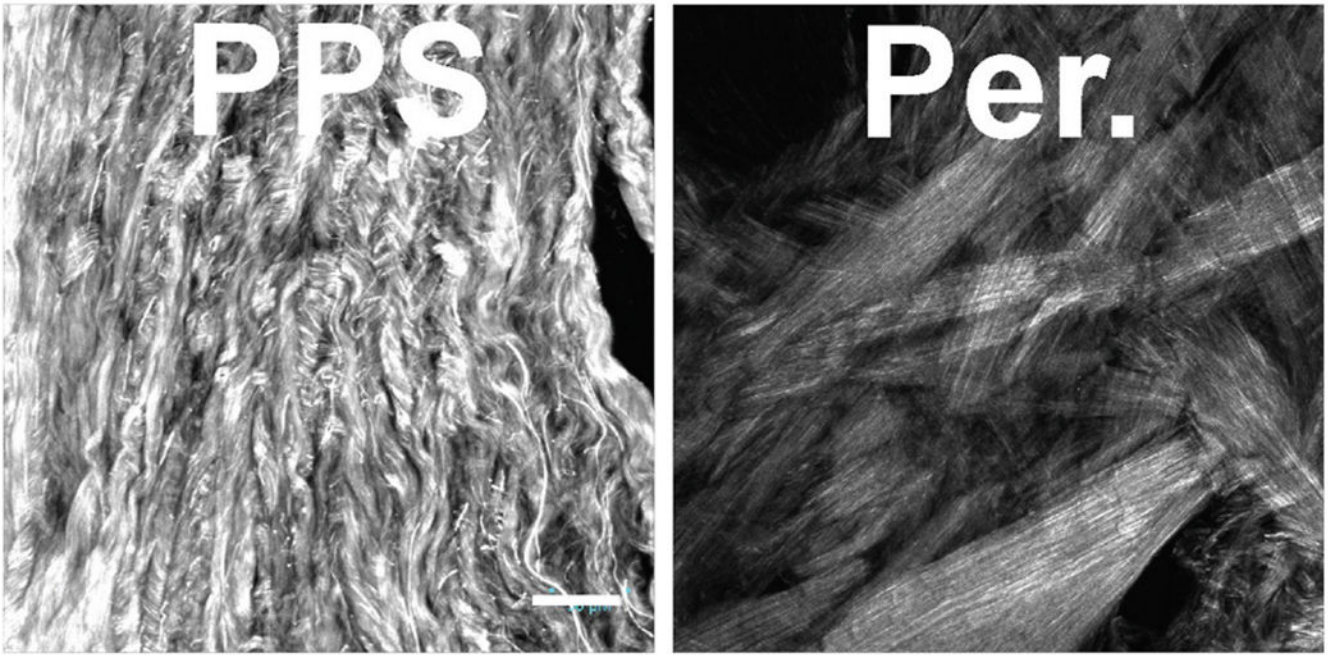

Fig. 3. Regionally specific collagen ultrastructure.

Second harmonic generation (SHG) imaging of collagen lamellae from a normal human eye. PPS collagen lamellae are highly aligned and arranged in a circumferential pattern around the optic nerve while peripheral (Per) collagen lamellae are organized in an interdigitated, basket-weave pattern (scale bar = 50 μm).

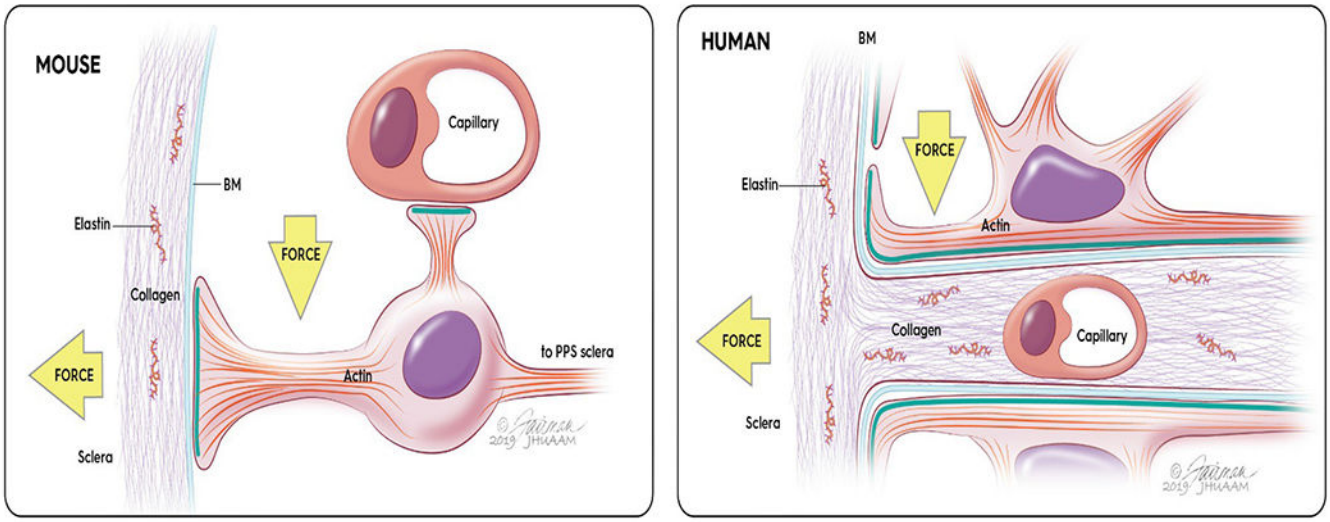

Fig. 4. IOP-induced strain is sensed at astrocyte-ECM junctional complexes.

Astrocytes in mouse ONH can span the diameter of the ON and have junctional complexes (green) consisting of integrin-linked transmembrane units connected to basement membrane produced by astrocytes that are adjacent to PPS and to capillaries. Human astrocytes reside on lamina connective tissue beams with similar junctional complexes. In both species, forces of translaminar pressure difference and centrifugal hoop stress are generated by IOP (arrows).

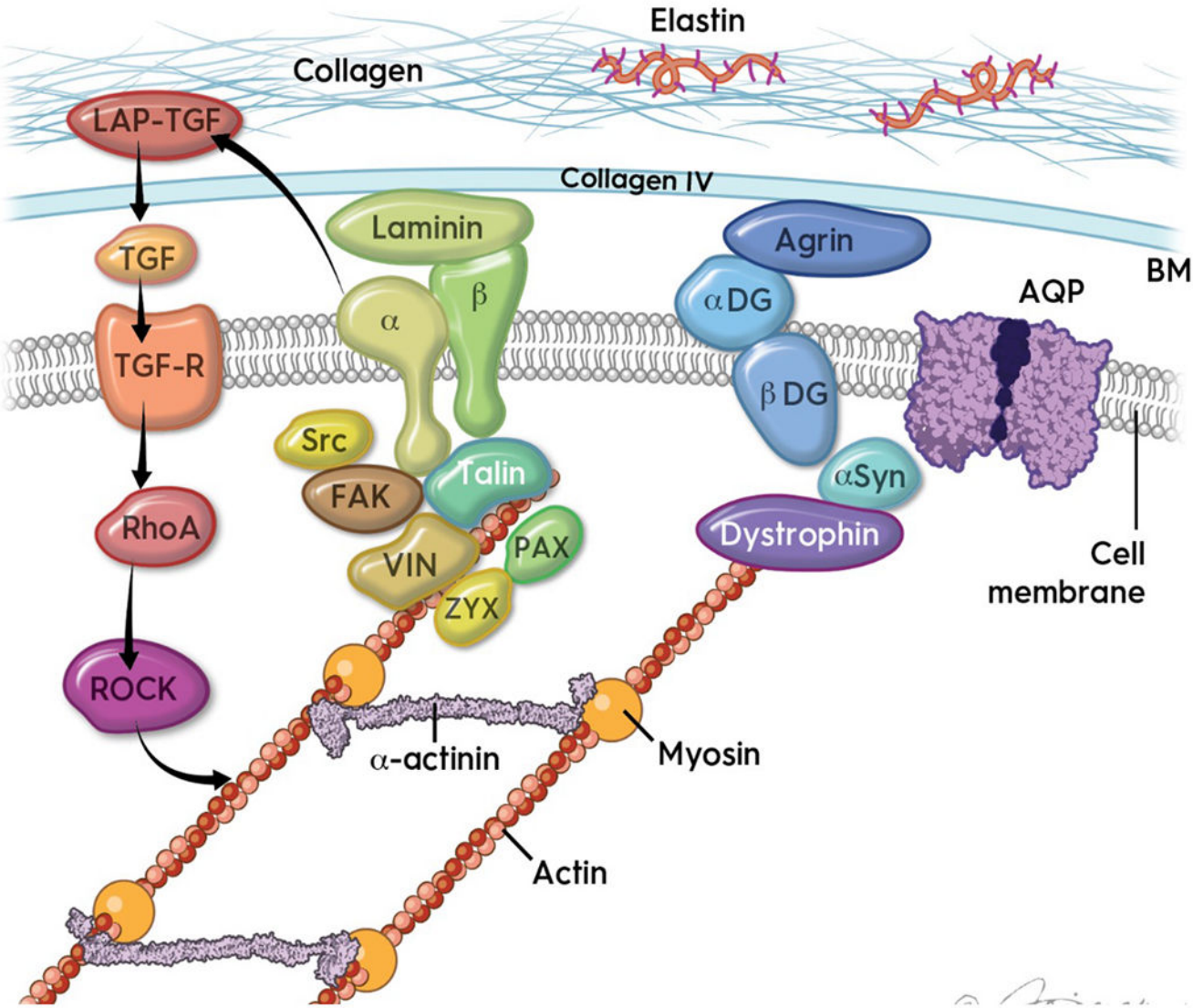

Fig. 5. Schematic simplification of complex junctional complex participants.

PPS collagen and elastin harbor latent TGFβ released by stress, signaling through α,β integrin in cell membrane attached to laminin. Pathway includes signaling by Src and FAK to talin, vinculin, zyxin and paxillin at the interface with actin filament network. Myosin and α-actinin form cytoskeletal networks altered by ROCK/RhoA stimulated by TGFβ. Astrocyte ONH junctions contain α,β-dystroglycan, typically attached to agrin in PPS and signaling to cytoskeleton through α-syntrophin & dystrophin. AQP channels, where present, require presence of dystroglycan.

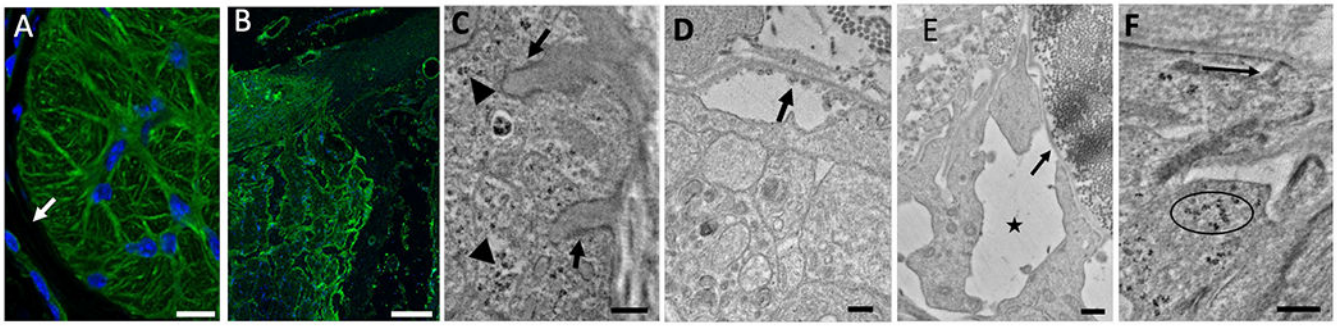

Fig. 6. Astrocyte response to IOP elevation.

(A) Mouse normal ONH with astrocytes labeled for integrin β1 (green) throughout cytoplasm and at end feet contacting PPS (arrow). (B) Normal human longitudinal section of ONH (integrin β1-green). (C): Mouse ONH at PPS, TEM junctional complex density (arrows) adjoins BM with integrin β1 immunogold label (arrowheads). After IOP elevation, astrocytes withdraw from BM at the PPS leaving remnants of astrocytes membrane still attached to their BM (arrow) (D). Mouse glaucoma 1w astrocytes withdraw from BM at PPS, leaving abnormal spaces, and E: withdraw junctional complex densities from membrane (arrow), with free α-dystroglycan identified by immunogold particles (circle) (E,F). Scale Bar-A: 10 μm, B: 50 μm, C,D,E,F: 200 nm.

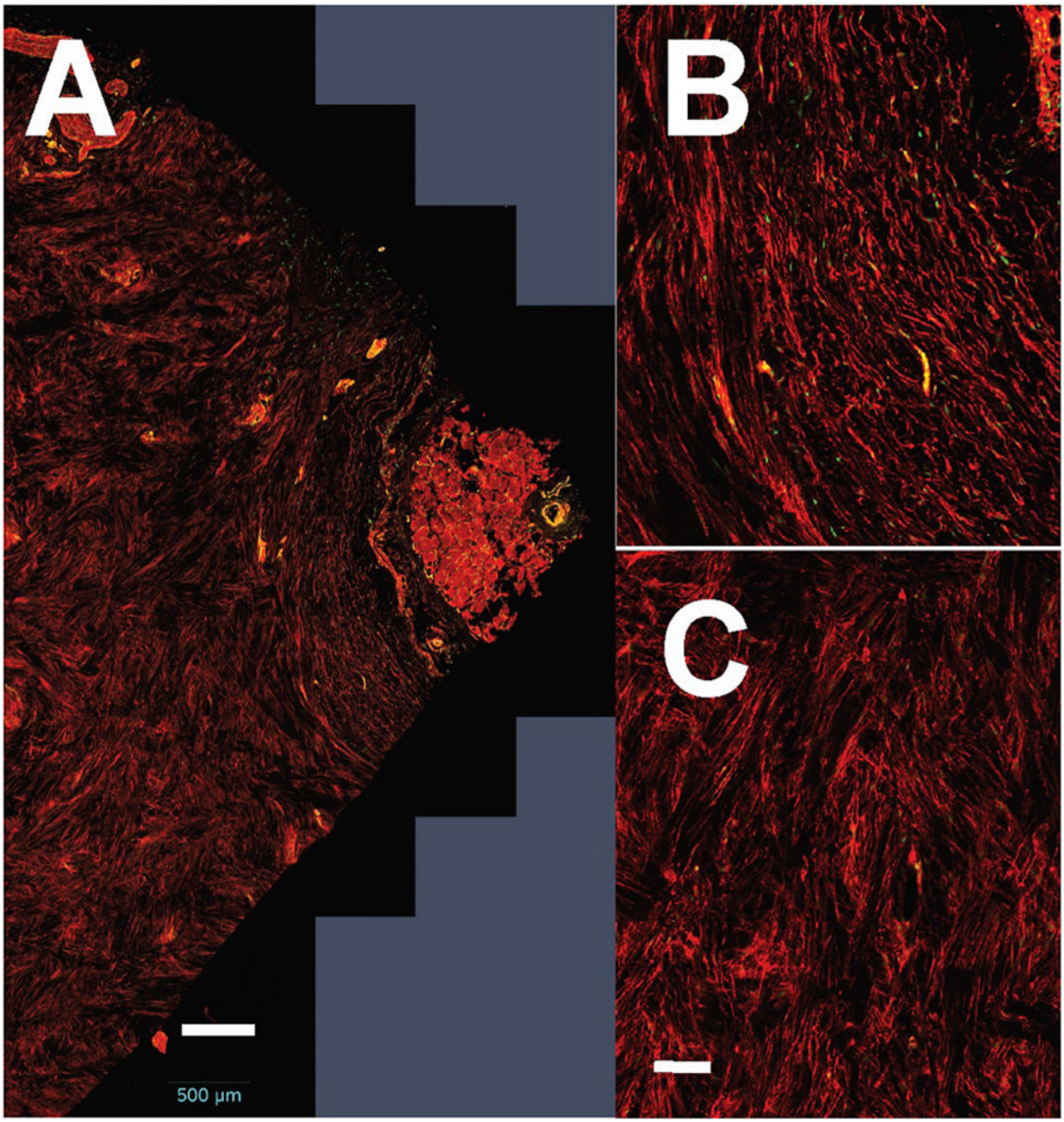

Fig. 7. Complex cytoskeletal organization and cellular morphology of scleral stromal fibroblasts.

(A) Cross section of a normal human optic nerve (right), PPS, and peripheral sclera (left) with phalloidin labelling of filamentous actin (red) shows actin organized circumferentially in the PPS (B) and in a basket-weave patter peripherally (C) (scale bar = 500 μm (A), 100 μm (B,C)).